Tetrahedron 65 (2009) 7718–7729

Contents lists available at ScienceDirect

Tetrahedron

journal homepage: www.elsevier.com/locate/tet

Hydrogen bonding-mediated foldamer-bridged zinc porphyrin-C_{60} dyads: ideal face-to-face orientation and tunable donor–acceptor interacion

Kui Wang [a], Yi-Shi Wu [b], Gui-Tao Wang [a], Ren-Xiao Wang [a], Xi-Kui Jiang [a], Hong-Bing Fu [b,*], Zhan-Ting Li [a,*]

[a] State Key Laboratory of Bioorganic and Natural Products Chemistry, Shanghai Institute of Organic Chemistry, Chinese Academy of Sciences, 345 Lingling Lu, Shanghai 200032, China
[b] Beijing National Laboratory for Molecular Sciences (BNLMS) and Institute of Chemistry, Chinese Academy of Sciences, Beijing 100190, China

ARTICLE INFO

Article history:
Received 6 May 2009
Received in revised form 15 June 2009
Accepted 19 June 2009
Available online 26 June 2009

Keywords:
Foldamer
Hydrogen bonding
Porphyrin
C_{60}
Charge transfer
Fluorescence
UV–Vis absorption

ABSTRACT

Four porphyrin-bridge-C_{60} dyads have been synthesized by covalently linking the chromophores at the opposite ends of a hydrogen bonded arylamide-derived foldamer bridge. For comparison, four C_{60}-free porphyrin derivatives of the same frameworks have also been prepared. The fully hydrogen bonded bridges enable the appended porphyrin and C_{60} moieties to contact in a face-to-face manner. ^{1}H NMR, UV–vis and fluorescent investigations in chloroform indicate that such a structural matching remarkably facilitates the intramolecular energy and electron transfer and charge separation between the two chromophores and also retards the recombination of the charge-separated state. Removing one hydrogen bond considerably reduces the energy and electron transfer. Further removing another one leads to no important interaction between the chromophores to occur.

1. Introduction

In the past decades, the development of porphyrin-C_{60} dyads have received considerable attention due to their rich redox, optical and photochemical properties.[1] A major consideration in the design of the porphyrin-C_{60} dyads is the overall molecular topology, mainly concerning their distance and spatial orientation,[2] which plays a crucial role in controlling the rate of the photoinduced electron transfer (PET), the efficiency of charge separation (CS) and the lifetime of the CS state. Both theory and experiment indicate that, when structurally possible, the dyads prefer to adopt a face-to-face conformation to maximize the interaction between the two chromophores and to favor the through-space donor–acceptor dialogues such as efficient and rapid quenching of the porphyrin fluorescence, generation of the C_{60} excited state and the charge transfer state.[3–5] However, accurate control of such an orientation has been a challenge synthetically.[6–14]

In the past decade, there has been a considerable interest in foldamers, linear molecules that are induced by noncovalent forces to adopt a specific secondary structure.[15–17] Among others,[18] hydrogen bonded oligoamide foldamers have been established as useful frameworks for controlling the interactions between functional segments.[17,19] A number of artificial receptors have been developed to bind ionic or neutral molecules or even protein surfaces.[20–22] Recently, quinoline-derived foldamers have been used as rigid linkers to regulate the photoinduced charge transfer between the two connected oligo(*p*-phenylene vinylene) and perylene bisimide chromophores.[23] We herein describe a new class of arylamide foldamer-derived zinc porphyrin-C_{60} dyads. The rigidity of the linkers enables the appended chromophores to orientate in a face-to-face manner. As a result, the photophysical process between the two chromophores can be tuned remarkably by simply controlling the number of the hydrogen bonds.

2. Results and discussion

2.1. Design and synthesis

Four porphyrin-C_{60} dyads **1**–**4** have been synthesized. The design was based on the recent observation that hydrogen bonded arylamide oligomers can form stable secondary structures.[16c,d,17] Compounds **1** and **2** were expected to form six hydrogen bonds to drive their arylamide bridge to adopt a rigid crescent conformation and thus to induce the two appended chromophores to arrange in a face-to-face manner. CPK modeling showed that keeping the six hydrogen bonds within the plane of their arylamide backbones

* Corresponding authors. Tel.: +86 21 54925122; fax: +86 21 64166128.
E-mail addresses: hongbing.fu@iccas.ac.cn (H.-B. Fu), ztli@mail.sioc.ac.cn (Z.-T. Li).

0040-4020/$ – see front matter © 2009 Elsevier Ltd. All rights reserved.
doi:10.1016/j.tet.2009.06.087

would force the two chromophores to contact closely. Therefore, it was envisioned that strong donor–acceptor interaction would occur between them. Compounds **3** and **4** have five and four hydrogen bonds, respectively. Their flexibility should be increasingly high. Owing to the inherent conjugation of the arylamide unit, **3** and **4** should mainly have two and four low-energy conformations, depending on the rotation of the amide relative to the appended benzene rings (see the structures). Except that one similar to that of **1**, their another one and three conformations would lead to long-distance separation for the porphyrin and C_{60} moieties. A comparison of their photophysical properties with those of **1** would reveal the influence of the hydrogen bonds. Compounds **5**–**9** were prepared as control compounds.

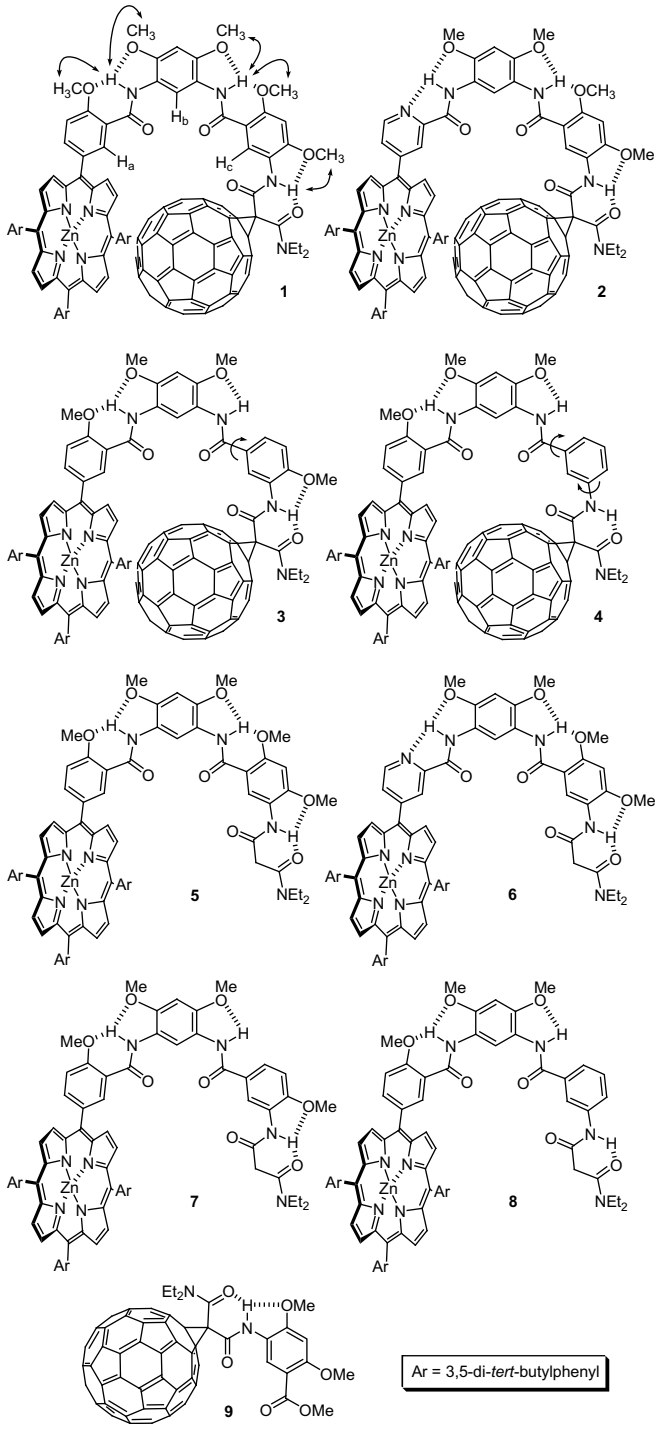

The synthetic route for **1** is shown in Scheme 1. Thus, **13** was first prepared in 3% yield from the reaction of **10**,[24] **11**[25] and **12** in refluxed $EtCO_2H$.[26] Hydrolysis of **13** with NaOH in refluxed pyridine afforded **14**, which was further treated with $SOCl_2$ in CH_2Cl_2 to yield **15**. With **15** in hand, **17** was prepared by palladium-catalyzed hydrogenation of **16**[27] in THF and then coupled with **18**[28] in CH_2Cl_2 in the presence of EDCI to yield **19** in 87% yield. This ester was further hydrolyzed to **20**, which was then reacted with **21**[29] in $CHCl_3$ to produce **22** in 76% yield. Further treatment of **22** with **15** in CH_2Cl_2 afforded **23** in 83% yield. The latter underwent the Bingel–Hirsch cyclopropanation in PhMe to afford **24** in 34% yield.[30] Finally, treatment of **24** with zinc acetate in CH_2Cl_2 and MeOH afforded **1** in 82% yield. Compounds **2**–**4** were prepared according to similar routes (Schemes 2–4). Compounds **5**–**8** were prepared by treating **23**, **29**, **35** and **41** with zinc acetate, while **9** was prepared from **19** via the Bingel–Hirsch cyclopropanation. All the compounds were characterized using ^1H and ^{13}C NMR spectroscopy and (high resolution) mass spectrometry.

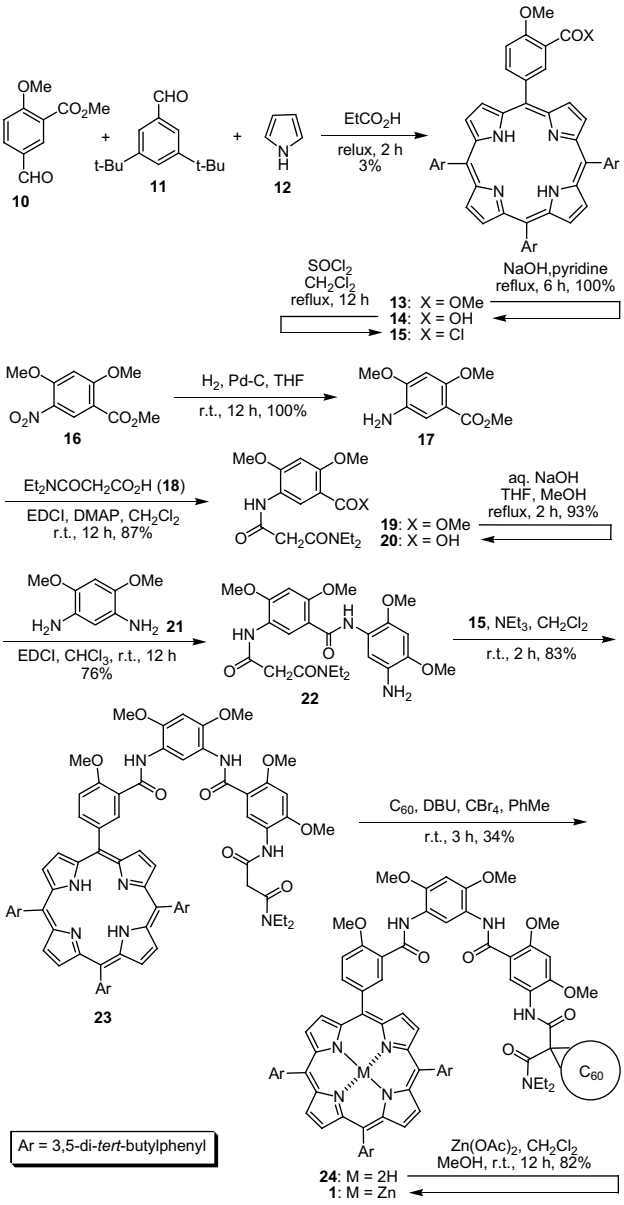

Scheme 1. The synthetic route for compound **1**.

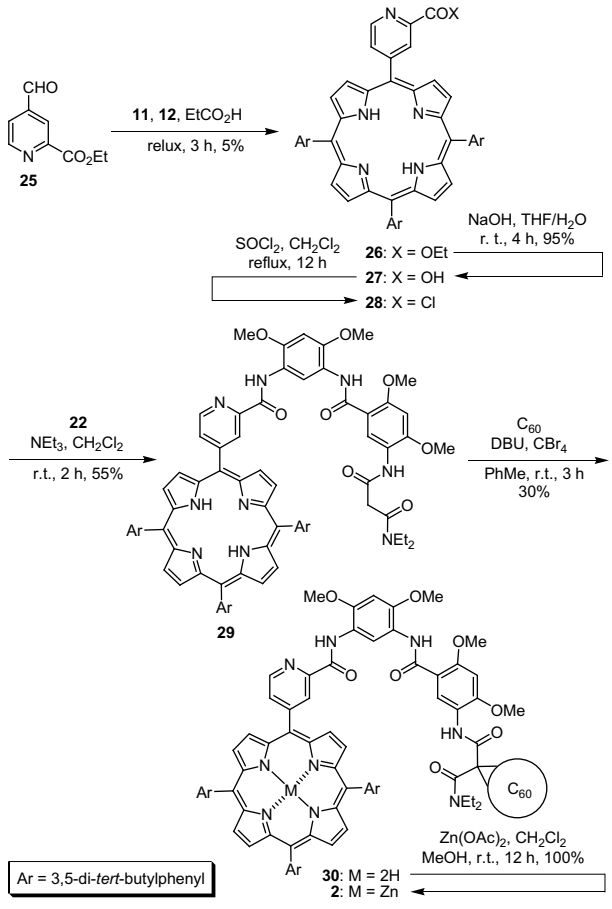

Scheme 2. The synthetic route for compound **2**.

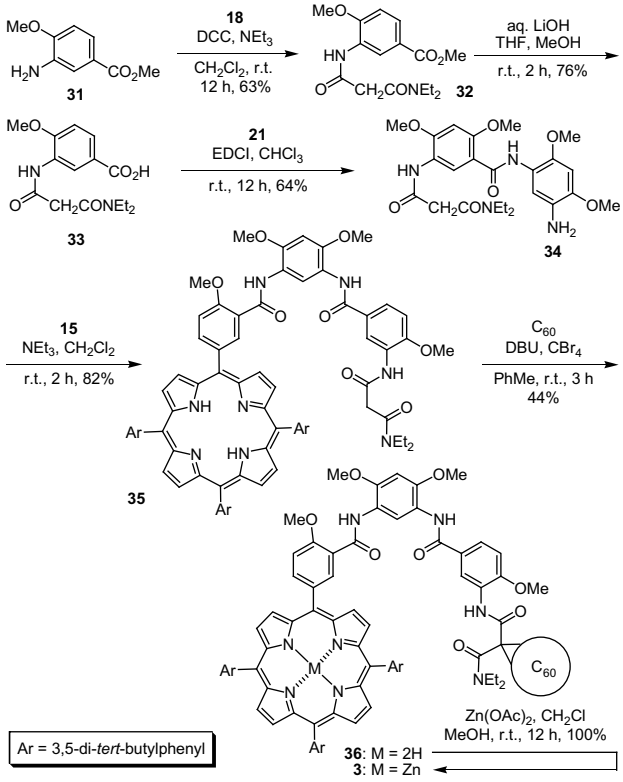

Scheme 3. The synthetic route for compound **3**.

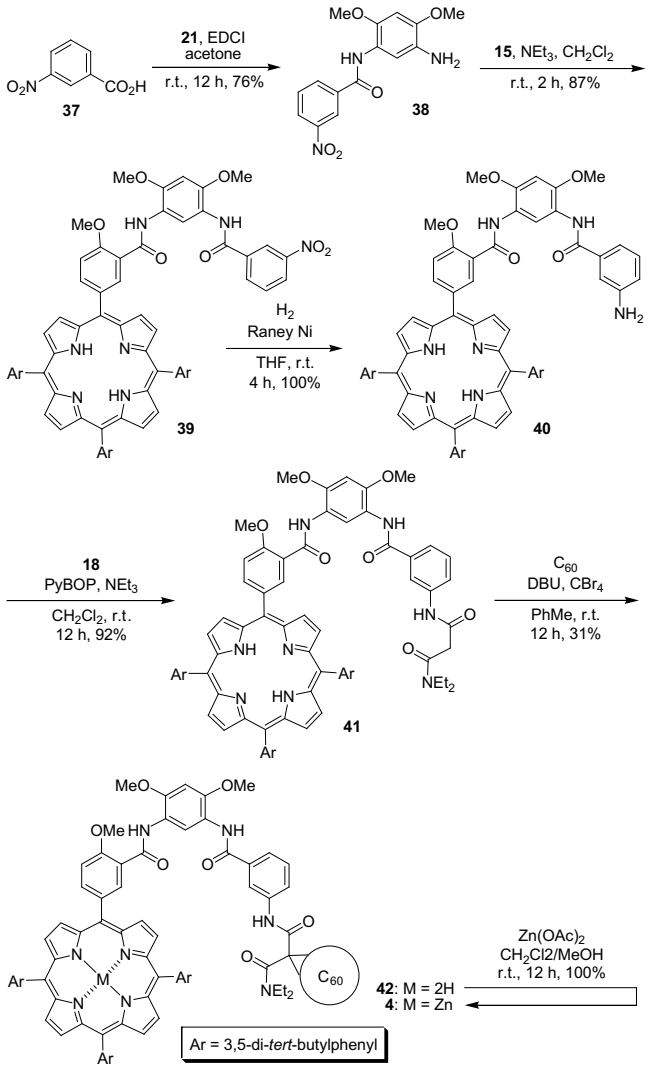

Scheme 4. The synthetic route for compound **4**.

2.2. ^{1}H NMR spectroscopy and hydrogen bonding

The hydrogen bonding in arylamide derivatives have been well-established.[16c,d,17] Because the porphyin and C_{60} moieties in compounds **1**–**4** are not close to the hydrogen bonding units, they should also form stable hydrogen bonding. The ^{1}H NMR spectra of **1**–**4** are shown in Figure 1. Actually, the signals of their amide hydrogens all appeared in the downfield area (>9.50 ppm for **1** and **2**) in the ^{1}H NMR spectra in $CDCl_3$, indicating that these hydrogens were indeed engaged in intramolecular hydrogen bonding. The NOESY spectrum of **1** in $CDCl_3$ exhibited strong NOEs between the amide hydrogens and the neighboring MeO hydrogens (see the structures). No similar connections were observed between the amide hydrogens and the related inner located hydrogens, i.e., H-a-c. These results also supported that the porphyrin and C_{60} moieties did not break the hydrogen bonding of the linker. Considering the high stability of the five membered N–H···N hydrogen bond in **2**,[16d] **2** should also form a similar folding conformation. ^{1}H NMR spectra also showed that the two chromophores of **1**–**4** approached each other, because comparing to those of their C_{60}-free counterparts **5** and **6** (Fig. 4), the signals of the hydrogens of the pyrroles and the benzenes at the *meso* positions of **1** and **2** shifted upfield or downfield pronouncedly, reflecting the shielding and de-shielding effects of the C_{60} moiety. Similar shifting was also exhibited for **3**

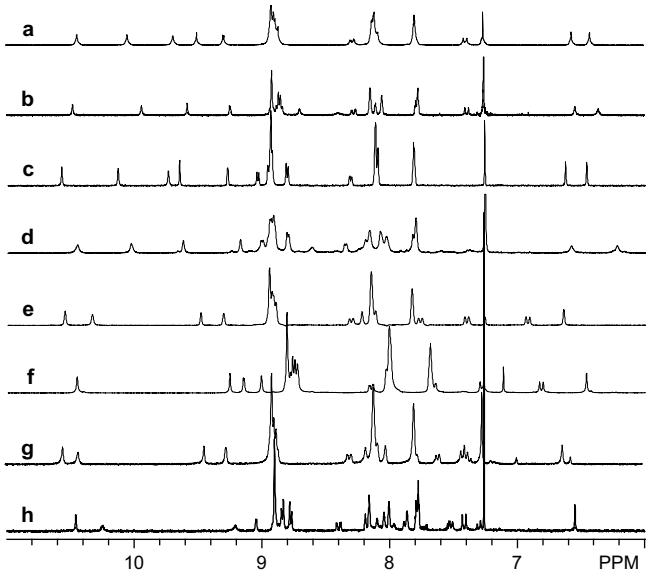

Figure 1. Partial ^{1}H NMR spectrum (300 MHz) of compounds (a) **5**, (b) **1**, (c) **6**, (d) **2**, (e) **7**, (f) **3**, (g) **8**, and (h) **4** in $CDCl_3$ (5 mM).

and **4** as compared with **7** and **8** (Fig. 1), suggesting that their C_{60} was also close to the porphyrin unit, albeit the linkers were increasingly flexible with the decrease of the number of the hydrogen bonds.

2.3. Crystal structures

To further evaluate the stability of the hydrogen bonding motif of the malonamide segment, we also prepared **44** and **46** from the reactions of **22** with **43** and **17** with **45**, respectively (Scheme 5). Their crystal structures were obtained and are provided in Figure 2. It can be found that the molonamide hydrogens of both compounds were all engaged in the three-center hydrogen bonding. As expected, the hydrogen bond of the terminal amide oxygen of **46** was remarkably weaker than the identical one in **44** due to the steric hindrance between its diethylamino unit and the neighboring methylene unit. Another amide of **46** was roughly perpendicular to the cyclopropane plane, suggesting that, even in the absence of the donor–acceptor interaction, the C_{60} in **1** and **2** should be located toward their porphyrin unit in a face-to-face manner due to the tendency of the backbones to form the intramolecular hydrogen bonding. These results are well consistent with the above ^{1}H NMR investigations, indicating that the new hydrogen bonded linkers are efficient in controlling the three dimensional orientation of the two chromophores.

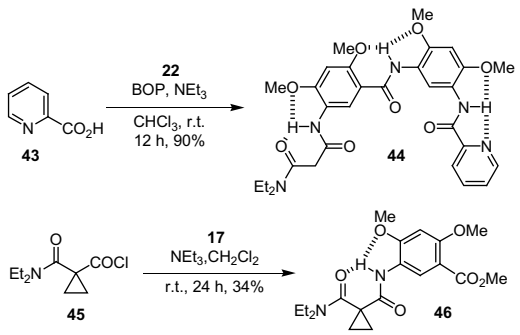

Scheme 5. The synthetic route for compounds **44** and **46**.

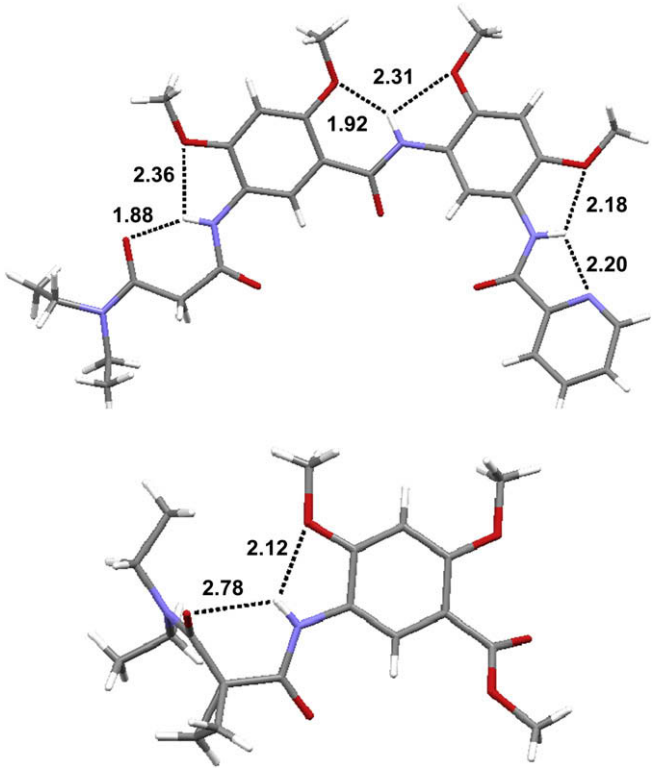

Figure 2. The crystal structures of compounds **44** (upper) and **46** (down), highlighting the three-center hydrogen bonding of the aryl amide backbones.

2.4. Steady-state absorption spectroscopy

The absorption spectra of **1**–**9** in $CHCl_3$ are provided in Figure 3. The absorption in the visible area was dominated by the porphyrin bands. The porphyrin moiety of **1** exhibited the typical Soret band (422 nm) and Q-bands (549 and 587 nm), while the porphyrin of **5** featured maxima at 423, 549 and 587 nm (Fig. 3a). Although, comparing to that of **5**, the Soret band of **1** was blue-shifted only by 1 nm, the molar absorption coefficient was decreased by 44%. Similar weakening (by 37%) was also observed for **2** as compared to **6**. These results clearly indicate that considerable photoinduced electron transfer occurred between the chromophores.[6,8] Because the porphyrin of **2** was attached to the electron-withdrawing pyridine, the values did not reflect the difference of the structural matching of **1** and **2**. Comparing to that of **7** and **8**, which lack the C_{60} moiety, the molecular absorption coefficient of the Soret band of **3** and **4** was reduced by 16% and 2%. The result indicates that the intramolecular hydrogen bonding played a crucial role in driving the two chromophores together, while the fully hydrogen bonded frameworks maximized this through a fully defined conformation.

2.5. Steady-state fluorescence spectroscopy

The emission spectra of the dyads and their porphyrin counterparts were measured in $CHCl_3$ at the 431 nm excitation wavelength, at which their molar absorption coefficients were identical (Fig. 4). Both **1** and **5** displayed fluorescence maxima at 598 and 643 nm, but the porphyrin emission of **1** was remarkably quenched by the attached C_{60} by a factor of 4.7. Similar quenching was also observed for **2**–**4** (by a factor of 3.3, 0.8 and 0.2) by comparing their emission with that of the C_{60}-free counterparts **6**–**8**. The quenching efficiency was quickly reduced with the decrease of the number of the hydrogen bonds. This is consistent with the above UV–vis result, showing that the linker of **1** and **2** most efficiently located the C_{60} at above the porphyrin moiety to enable rapid quenching of the

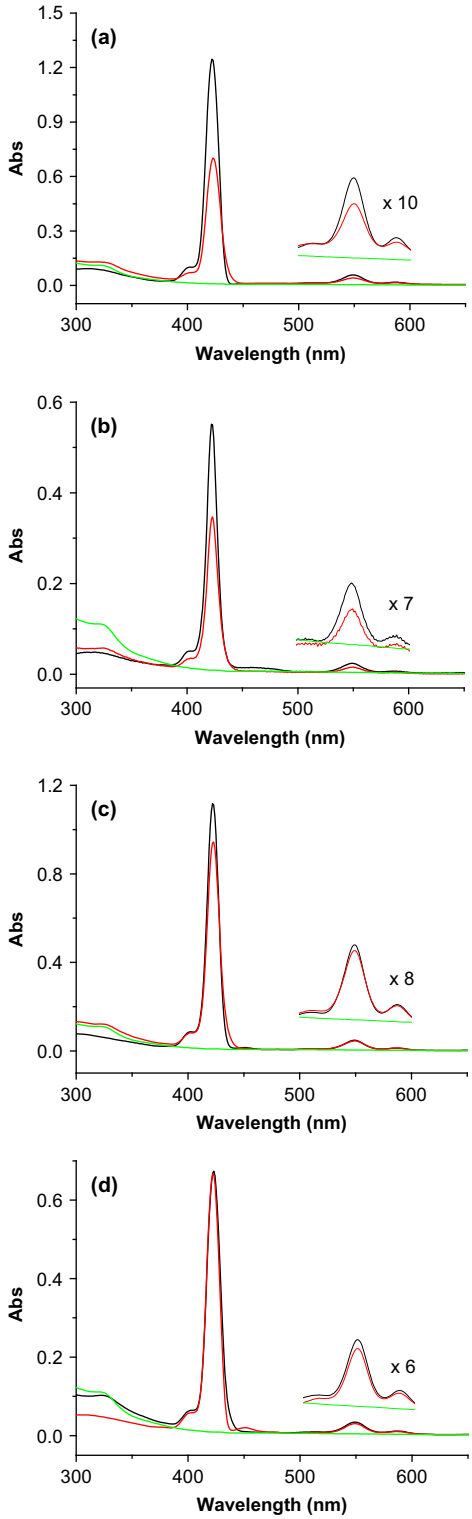

Figure 3. UV–vis absorption spectra in chloroform at 25°C: (a) **1** (black), **5** (red) and **9** (green), (b) **2** (black), **6** (red) and **9** (green), (c) **3** (black), **7** (red) and **9** (green), and (d) **4** (black), **8** (red) and **9** (green). The concentration was 2.0×10^{-6} M for all the samples.

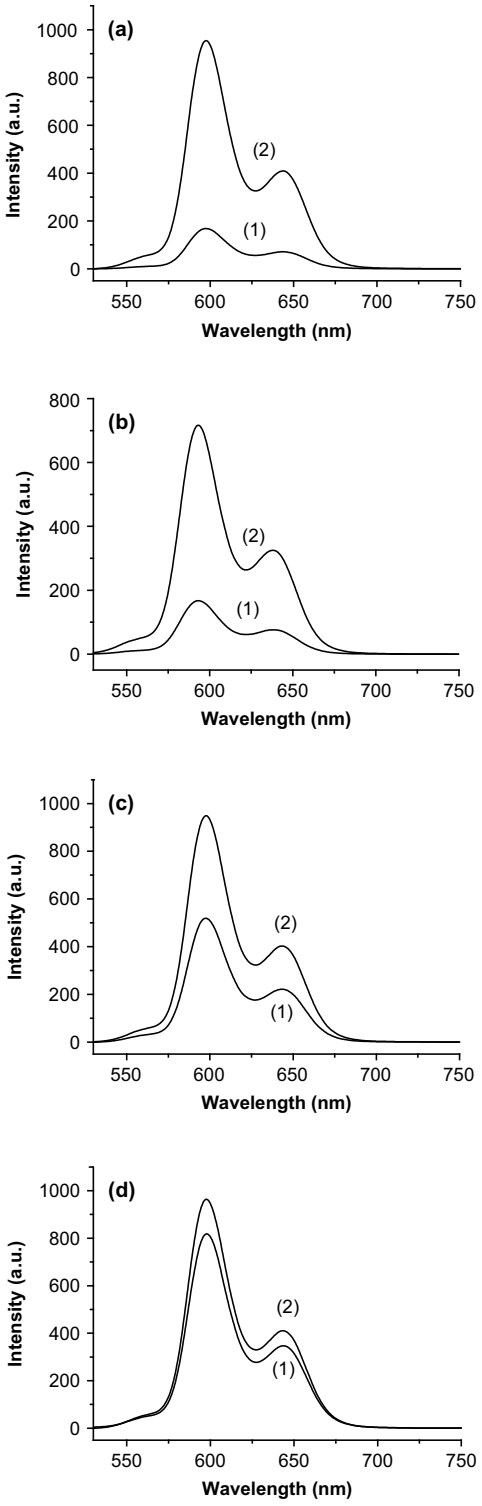

Figure 4. Fluorescent emission spectra in chloroform at 25°C with excitation at 431 nm: (a) 1 (1) and 5 (2), (b) 2 (1) and 6 (2), (c) 3 (1) and 7, and (d) 4 (1) and 8 (2). Concentrations were 2.0×10^{-6} M.

porphyrin excited singlet state. For dyads **1**–**4**, no C_{60} emission was detected in the range of 700–750 nm,[31] suggesting that no important singlet–singlet energy transfer from porphyrin to C_{60} occurred. Therefore, the quenching should be predominantly caused by the intramolecular electron transfer from the excited singlet state of porphyrin (P) to C_{60} to afford the $P^{\bullet+}/C_{60}^{\bullet-}$ charge-separated radical ion pair (CSRP).

The quenching efficiency of the porphyrin by the attached C_{60} in **1** and **2** is lower than that revealed for the cyclophane-based dyads in which the porphyrin and C_{60} moieties are held together by two flexible aliphatic chains.[7,9] It is reported that in these dyads the fluorescence of porphyrin is nearly completely quenched by the attached C_{60}. In these cyclophanes, the two chromophores approach each other mainly owing to the simple geometric matching,

together with their inherent donor–acceptor interaction. In the new foldamer-derived systems, without considering the inherent donor–acceptor interaction, the low-energy conformation is mainly controlled by the hydrogen bonds. Any re-orientation of the two chromophores due to and for the intramolecular energy and/or electron transfer would require a structural deviation from the minimum energy conformation controlled by the strong hydrogen bonding.

2.6. Time-resolved fluorescence studies

Picosecond time-resolved fluorescence experiments were carried out on **1**, **3** and **4** and C_{60}-free **5**, **7** and **8** in $CHCl_3$ to further study the effect of the conformational organization on the photo-induced electron transfer in the dyads. For comparison, all the solutions were excited at 540 nm, and the emission decay profiles were collected at 597 nm. The results are listed in Table 1. The time profiles of **1**, **3** and **4** can be well-fitted with a bi-exponential function (Fig. 5). Their lifetimes τ_{f1} and τ_{f2} were evaluated by the curve-fitting method. The fast-decaying component (150 ps for **1**, 260 ps for **3** and 280 ps for **4**, respectively) can be assignable to the decay of excited zincporphyrin as a result of electron transfer from it to C_{60}. The second decay component may be produced from $P^{\bullet+}/C_{60}^{\bullet-}$ by direct electron transfer from $^1P^*$ to C_{60} or the singlet–singlet energy transfer to give $^1C_{60}^*$ followed by electron transfer. Since no evidence was obtained for the formation of $^1C_{60}^*$, it should be reasonable to assign it to an equilibration between $^1P^*$ and the CSRP state.[32] Both τ_{f1} and τ_{f2} values are increased from **1** to **3** and to **4**, which is consistent with the above steady-state absorption and fluorescence observations, again reflecting the effect of the intramolecular hydrogen bonding on the structural preorganization. The close contact favored both decaying processes, leading to the shorter lifetimes for **1**.

The shorter-lived component has large amplitude (0.57) for **1**, small amplitude (0.31) for **3** and average amplitude (0.50) for **4**, which may be rationalized by considering the conformational complexity of the hydrogen bonded dyads. Removal of a hydrogen bond would not only increase the flexibility of the skeleton, but also cause variations on the bond length and angle of the concerned amide group. Both changes should not be linear with the numbers of the hydrogen bonds, which may lead to the different amplitude. The fluorescence decay of **5**, **7** and **8** was well-fitted with a single-exponential decay function. Their lifetimes τ_{f1} are comparable, which can be assigned to the excited porphyrin. This observation shows that the C_{60}-free linker has no important impact on the fluorescence decay. The charge separation (CS) rates from $^1P^*$ to C_{60} for **1**, **3** and **4** were determined from the following equation by using the fluorescence lifetimes: $k_{cs}=1/\tau_{f1}-1/\tau_{fr}$ (Table 1). It can be found that the rate was reduced pronouncedly with the decrease of the hydrogen bonds on the linker, reflecting the increase of the structural flexibility from **1** to **3** and then to **4**. The related quantum yields (Φ_{CS}) were obtained from the equation: $\Phi_{CS}=1-(\tau_{f1}/\tau_{fr})$ (Table 1). The Φ_{CS} is high for all the three dyads, implying that their C_{60} moiety is still close to the porphyrin moiety for the charge separation process to occur, while the highest Φ_{CS} exhibited by **1** supports that this dyad possesses the most matched relative orientation between the two chromophores.

Table 1
The PET procedure parameters of **1**, **3**, **4**, **5**, **7**, and **8** in $CHCl_3$[a,b]

Comp	τ_{f1} (ps)	τ_{f2} (ps)	τ_{fr} (ps)	k_{CS} (s^{-1})	Φ_{CS}
1	150 (0.57)	610 (0.43)		6.1×10^9	0.92
5			1790		
3	260 (0.31)	980 (0.69)		3.2×10^9	0.82
7			1440		
4	280 (0.50)	1310 (0.50)		2.9×10^9	0.82
8			1570		

[a] λ_{exc}=540 nm, λ_{obs}=597 nm, concentrations were 2.0×10^{-5} M for all the samples.
[b] Values in parentheses are relative amplitudes.

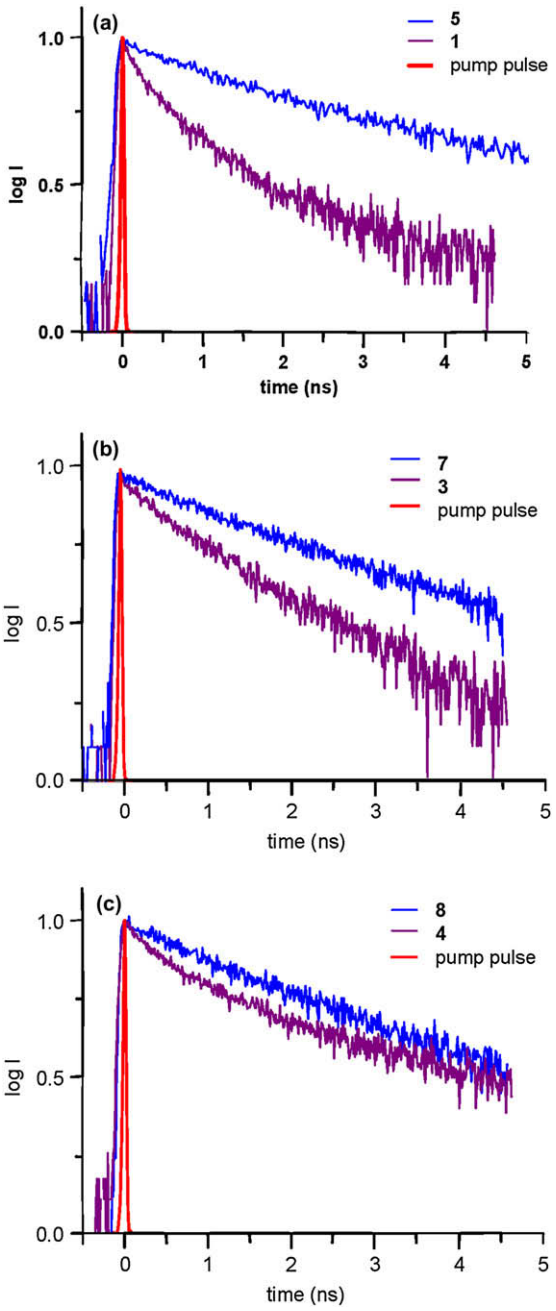

Figure 5. Time profiles of the fluorescence of (a) **1** (purple) and **5** (blue), (b) **3** (purple) and **7** (blue), and (c) **4** (purple) and **8** (blue) in chloroform at 597 nm upon excitation at 540 nm. Concentrations were 2.0×10^{-5} M and the red was pump pulse.

2.7. Time-resolved absorption studies

To shed more light on the ET process, time-resolved transient spectra of **1**, **3** and **4** in $CHCl_3$ were measured by femtosecond laser photolysis with excitation wavelength at 400 nm for selective photoexcitation of zincporphyrin. Global analysis was employed on twenty kinetic traces within the spectral range of 970–1160 nm, leading to two decay components, as shown in Figure 6. The decay

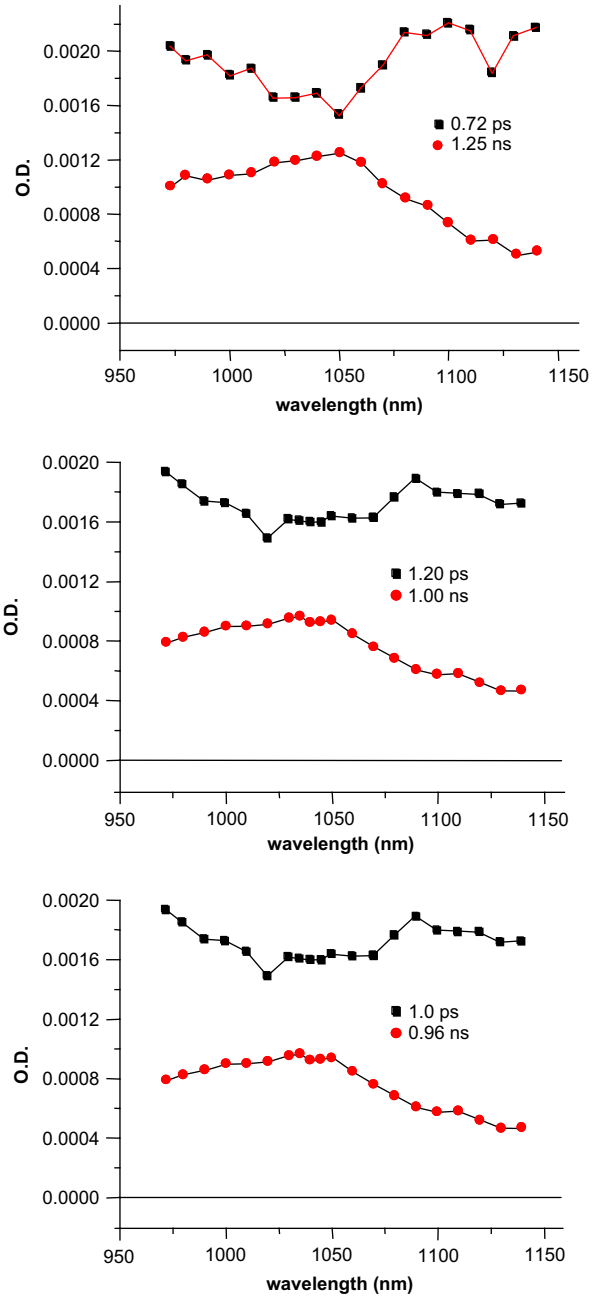

Figure 6. Decay associated spectra obtained from global analysis on several representive kinetic traces within the range of 970–1150 nm recorded on the 1600 ps time scale.

associated spectra (DAS) of the short components share a similar feature, assignable to the excited zincporphyrin. All the DAS of the three dyads exhibited broad absorption band centered about 1040 nm, which is characteristic of the C_{60} radical anion. Therefore, the charge recombination process can be evaluated with time constants of 8.0×10^8 (for **1**), 1.0×10^9 (for **3**) and 1.1×10^9 (for **4**) s^{-1}. It can be found that the values are decreased notably, indicating that the charge-recombination rate becomes quicker when the rigidity of the arylamide framework is reduced. This study, together with the above transient fluorescence studies, reveals that the fully hydrogen bonded dyad **1** not only favors the charge transfer, but also retards the charge recombination, impling that the charge recombination in **1** has been pushed into the Marcus inverted region.[33]

3. Conclusions

We have demonstrated that the hydrogen bonded arylamide foldamer is a useful linker to control the relative orientation and consequently the energy and electron transfer of the porphyrin and C_{60} moieties. Considering that many donor–acceptor systems have been established, the porphyrin and C_{60} moieties in the present dyads can be readily replaced with other electron donors or acceptors. The shape of the frameworks can also be readily regulated by simply changing the position of the substituents for the hydrogen bonding. Therefore, this approach may be developed as a general strategy to tune the photophysical properties of dyads or even triads. Since the charge recombination rate of **1** is retarded in the fully hydrogen bonded architecture, we may expect longer lifetime of charge separation if another C_{60} or porphyrin moiety is introduced to form a similar triad or more complexed systems. Therefore, the work opens many possibilities for the development of new functional molecules and materials.

4. Experimental section

4.1. General methods

See Ref. 20b.

4.2. Time-resolved fluorescence experiments

The measurements were carried out on the ps time-resolved fluorescence spectrometer. The 540-nm laser pulses were generated from a Ti:sapphire regenerative amplifier and used as the excitation pulses. The pulse energy was about 100 nJ/pulse at the sample. Fluorescence gathered with the 90-degree-geometry was dispersed by a polychromator and collected with a photon-counting type streak camera. The data detected by digital camera is rountinely transferred to PC for analysis with HPDTA software. The spectral resolution was 0.2 nm and the temporal resolution was 2–100 ps depending on the delay-time-range setting.

4.3. Time-resolved absorption experiments

The 800-nm laser pulses generated from a Ti:sapphire regenerative amplifier were frequency doubled and used as the pump pulses. The residual 800-nm pulses were further attenuated and focused into a 3-mm sapphire plate to generate the probe pulses. The time delay between the pump and probe beams were regulated through a computer-controlled motorized translation stage in the probe beam. A magic-angle scheme was adopted in the pump-probe measurement. The temporal resolution between the pump and the probe pulses was determined to be ~150 fs (FWHM). The transmitted light was detected by an InGaAs linear image sensor. The excitation pulsed energy was 0.2 μJ/pulse as measured at the rotating sample cell (optical path length 1 mm). A typical absorbance of 0.4–0.8 at the excitation wavelength was used. The stability of the solutions was spectrophotometrically checked before and after each experiment. Analysis of the kinetic traces derived from time-resolved spectra was performed individually and globally using nonlinear least-square fitting to a general sum-of-exponentials function after deconvolution of instrument response function (IRF). Decay-associated spectra (DAS) were acquired from global analysis of some representative kinetic traces at selected wavelengths. All the spectroscopic measurements were carried out at room temperature.

4.4. Compound 13

To a solution of **10** (10.6 g, 55.0 mmol) and **11** (36.0 g, 0.17 mol) in refluxed $EtCO_2H$ (500 mL) was added pyrrole **12** (15.3 mL,

0.22 mol) in 0.5 h. The solution was refluxed for 2 h and then concentrated. The resulting residue was dissolved in toluene (200 mL) and the solution concentrated again. This process was repeated for three times and the resulting slurry subjected to column chromatography (CH_2Cl_2/*n*-hexane 1:1) to give **13** as a purple solid (1.88 g, 3%). ^{1}H NMR (300 MHz, $CDCl_3$): δ 9.08 (d, J=2.4 Hz, 1H), 8.91 (s, 6H), 8.83 (d, J=4.8 Hz, 2H), 8.68 (d, J=2.4 Hz, 1H), 8.32 (dd, J_1=8.1 Hz, J_2=2.1 Hz, 6H), 8.10–8.06 (m, 6H), 7.80–7.76 (m, 3H), 7.38 (d, J=8.7 Hz, 1H), 4.21 (s, 3H), 3.91 (s, 3H), 1.52 (s, 64H), −2.73 (s, 2H). MS (MALDI-TOF): m/z 1040 $[M+H]^+$. Anal. Calcd for $C_{71}H_{82}N_4O_3$: C, 82.04; H, 7.95; N, 4.62. Found: C, 82.05; H, 8.08; N, 5.15.

4.5. Compound 26

^{1}H NMR (300 MHz, $CDCl_3$): δ 9.18 (d, J=4.6 Hz, 1H), 9.02 (s, 1H), 8.93 (d, J=8.8 Hz, 6H), 8.72 (d, J=4.7 Hz, 2H), 8.35 (d, J=4.8 Hz, 1H), 8.08 (s, 6H), 7.81 (d, J=1.2 Hz, 3H), 4.59 (q, J=7.1 Hz, 2H), 1.55–1.51 (m, 57H), −2.70 (s, 2H). ^{13}C NMR (100 MHz, $CDCl_3$): δ 165.6, 152.3, 148.9, 148.8, 148.3, 146.9, 141.1, 141.0, 132.0, 130.2, 129.8, 129.7, 122.6, 122.0, 121.2, 114.6, 62.2, 35.1, 31.8, 31.5, 14.4. MS (MALDI-TOF): m/z 1024.8 $[M+H]^+$. HRMS (MALDI-FT): Calcd for $C_{70}H_{82}N_5O_2$ $[M+H]^+$: 1024.6472. Found: 1024.6463.

4.6. Compound 14

A solution of **13** (0.10 g, 0.10 mmol) and NaOH (20 mg, 0.50 mmol) in pyridine (20 mL) and water (4 mL) was heated under reflux for 6 h and then concentrated with a rotavapor. The resulting slurry was treated with diluted HCl (0.5 mL) to pH=3 and then the mixture extracted with CH_2Cl_2 (10 mL). The organic phase was washed with water (10 mL) and brine (10 mL), and dried over sodium sulfate. Removal of the solvent under reduced pressure afforded **14** as a purple solid (0.10 g, 100%). ^{1}H NMR (300 MHz, $CDCl_3$): δ 8.91 (s, 6H), 8.83 (d, J=4.8 Hz, 2H), 8.92–8.88 (m, 6H), 8.76 (d, J=4.8 Hz, 2H), 8.43 (dd, J_1=8.6 Hz, J_2=2.7 Hz, 1H), 8.10–8.07 (m, 6H), 7.82–7.78 (m, 3H), 7.47 (d, J=8.7 Hz, 1H), 4.38 (s, 3H), 1.53 (s, 54H), −2.73 (s, 2H). ^{13}C NMR (100 MHz, $CDCl_3$): δ 165.8, 157.8, 149.0, 148.8, 141.3, 141.2, 140.0, 138.5, 136.6, 130.0, 129.8, 129.7, 121.9, 121.7, 121.1, 117.0, 116.2, 110.1, 56.9, 35.1, 31.8. MS (MALDI-TOF): m/z 1026 $[M+H]^+$. Anal. Calcd for $C_{70}H_{80}N_4O_3$: C, 81.99; H, 7.86; N, 5.46. Found: C, 81.47; H, 7.98; N, 5.08.

4.7. Compound 27

^{1}H NMR (300 MHz, $CDCl_3$): δ 9.18 (d, J=5.1 Hz, 1H), 9.03 (s, 1H), 8.96–8.93 (m, 6H), 8.74–8.72 (m, 2H), 8.36 (d, J=4.5 Hz, 1H), 8.09 (s, 6H), 7.82 (s, 3H), 1.54 (s, 54H), −2.70 (s, 2H). ^{13}C NMR (100 MHz, $CDCl_3$): δ 159.6, 148.9, 148.8, 141.1, 141.0, 129.9, 129.7, 122.8, 122.2, 121.2, 35.1, 32.1, 31.8, 31.5, 31.4, 30.4, 29.7. MS (MALDI-TOF): m/z 996.9 $[M+H]^+$. HRMS (MALDI-FT): Calcd for $C_{68}H_{78}N_5O_2$ $[M+H]^+$: 996.6125. Found: 996.6150.

4.8. Compound 19

A solution of **17** (1.59 g, 7.55 mmol), **18** (1.26 g, 7.93 mmol), EDCI (3.69 g, 8.31 mmol) and DMAP (50 mg, 0.4 mmol) in CH_2Cl_2 (50 mL) and NEt_3 (3.46 mL, 24.9 mmol) was stirred for 12 h and then washed with diluted aqueous HCl (0.5 N, 25 mL), water (2×25 mL) and brine (25 mL), and dried over sodium sulfate. Upon removal of the solvent with a rotavapor, the crude product was recrystallized from MeOH to give **19** as a white solid (2.31 g, 87%). ^{1}H NMR (300 MHz, $CDCl_3$): δ 10.15 (s, 1H), 8.79 (s, 1H), 6.50 (s, 1H), 3.98 (s, 3H), 3.92 (s, 3H), 3.85 (s, 3H), 3.47–3.36 (m, 6H), 1.24 (t, J=6.9 Hz, 3H), 1.17 (t, J=6.9 Hz, 3H). ^{13}C NMR (100 MHz, $CDCl_3$): δ 167.7, 165.7, 164.1, 157.5, 153.4, 124.0, 120.5, 111.4, 95.8, 56.5, 56.1, 51.7, 42.8, 40.9, 40.7, 14.4, 12.9. MS (EI): m/z 352 $[M]^+$. Anal. Calcd for $C_{17}H_{24}N_2O_6$: C, 57.94; H, 6.68; N, 7.95. Found: C, 57.69; H, 6.98; N, 7.49.

4.9. Compound 41

^{1}H NMR (300 MHz, $CDCl_3$): δ 10.55 (s, 1H), 10.43 (s, 1H), 9.44 (s, 1H), 9.27 (s, 1H), 8.91–8.87 (m, 8H), 8.30 (d, J=8.4 Hz, 1H), 8.20 (s, 1H), 8.14–8.10 (m, 6H), 7.82 (s, 4H), 7.63 (d, J=7.8 Hz, 1H), 7.42 (t, J=8.7 Hz, 2H), 6.65 (s, 1H), 4.36 (s, 3H), 4.07 (s, 3H), 3.96 (s, 3H), 3.44 (s, 2H), 3.42–3.33 (m, 4H), 1.56 (s, 54H), 1.24–1.09 (m, 6H), −2.66 (s, 2H). ^{13}C NMR (100 MHz, $CDCl_3$): δ 167.6, 164.8, 164.5, 162.5, 157.1, 148.8, 148.7, 148.6, 148.6, 146.3, 141.4, 141.3, 138.3, 136.1, 135.7, 130.0, 129.8, 129.7, 129.6, 129.2, 122.9, 122.8, 121.5, 121.4, 121.0, 120.8, 120.4, 118.5, 118.3, 115.5, 110.0, 95.6, 56.6, 56.4, 56.2, 42.6, 40.9, 39.9, 35.0, 32.3, 31.8, 31.5, 31.3 (d), 14.2, 12.8, 1.1. MS (MALDI-TOF): m/z 1437.0 $[M+H]^+$. HRMS (MALDI-FT): Calcd for $C_{92}H_{107}N_8O_7$ $[M+H]^+$: 1435.8246. Found: 1435.8257.

4.10. Compound 20

A solution of **19** (0.50 g, 1.42 mmol) and lithium hydroxide monohydrate (1.60 g, 15.2 mmol) in MeOH (200 mL) was stirred for 2 h and then concentrated with a rotavapor. The resulting slurry was added to water (10 mL). The mixture was acidified with diluted HCl to pH=2 and then extracted with $CHCl_3$ (20 mL×3). The organic phases were combined and washed with water (30 mL) and brine (30 mL), and dried over sodium sulfate. Removal of the solvent afforded **20** as a white solid (0.48 g, 100%). ^{1}H NMR (300 MHz, $CDCl_3$): δ 10.21 (s, 1H), 8.96 (s, 1H), 6.54 (s, 1H), 4.08 (s, 3H), 4.01 (s, 3H), 3.49–3.47 (m, 6H), 1.24 (t, J=7.5 Hz, 1H), 1.18 (t, J=7.5 Hz, 1H). MS (ESI): m/z 338 $[M]^+$. ^{13}C NMR (100 MHz, $CDCl_3$): δ 167.7, 164.9, 164.2, 155.8, 154.5, 125.5, 122.2, 109.7, 94.9, 57.0, 56.4, 42.8, 40.9, 40.5, 14.4, 12.9. Anal. Calcd for $C_{16}H_{22}N_2O_6$: C, 56.80; H, 6.55; N, 8.28. Found: C, 56.58; H, 6.69; N, 8.01.

4.11. Compound 22

A solution of **20** (0.32 g, 1.92 mmol), **21** (0.16 g, 0.48 mmol), EDCI (0.14 g, 0.72 mmol) and DMAP (80 mg) in $CHCl_3$ (100 mL) was stirred for 12 h and then washed with saturated aqueous $NaHCO_3$ (50 mL), water (50 mL×3) and brine (50 mL), and dried over sodium sulfate. The solvent was removed and the resulting residue subjected to column chromatography (CH_2Cl_2/MeOH, 50:1) to give **22** as a pale brown solid (0.14 g, 76%). ^{1}H NMR (300 MHz, $CDCl_3$): δ 10.24 (s, 1H), 9.99 (s, 1H), 8.98 (s, 1H), 8.17 (s, 1H), 6.51 (s, 1H), 6.51 (s, 1H), 4.04 (s, 3H), 3.97 (s, 3H), 3.88 (s, 3H), 3.84 (s, 3H), 3.48 (s, 2H), 3.44–3.40 (m, 4H), 1.22 (t, J=6.9 Hz, 3H), 1.17 (t, J=7.2 Hz, 3H). MS (ESI): m/z 489 $[M+H]^+$. ^{13}C NMR (100 MHz, $CDCl_3$): δ 167.9, 164.0, 162.1, 154.8, 153.1, 142.8, 141.4, 129.9, 125.0, 122.9, 121.4, 114.9, 108.6, 97.7, 95.2, 77.2, 57.3, 56.5, 56.2, 42.9, 40.9, 14.4, 13.0. MS-HR (MALDI-TOF-FT): Calcd for $C_{24}H_{32}N_4O_7Na$ $[M+Na]^+$: 511.2173. Found: 511.2163.

4.12. Compound 23

A solution of **14** (0.16 g, 0.15 mmol) and thionyl chloride (0.72 mL, 9.90 mmol) in CH_2Cl_2 (30 mL) was heated under reflux for 12 h and then concentrated under reduced pressure to afford **15** as dark green solid. The solid was dissolved in CH_2Cl_2 (30 mL) and the solution added to a stirred solution of **22** (78 mg, 0.15 mmol) and NEt_3 (0.06 mL, 0.51 mmol) in CH_2Cl_2 (30 mL). The solution was stirred for 2 h and then washed with diluted HCl (0.1 N, 30 mL), water (30 mL×2) and brine (30 mL), and dried over sodium sulfate. After the solvent was removed with a rotavapor, the resulting crude prude was subjected to flash chromatography (CH_2Cl_2/MeOH, 50:1) to give **5** as a purple solid (0.19 g, 83%). ^{1}H NMR (300 MHz, $CDCl_3$):

δ 10.43 (s, 1H), 10.04 (s, 1H), 9.68 (s, 1H), 9.49 (s, 1H), 9.28 (d, J=2.4 Hz, 1H), 8.91–8.85 (m, 9H), 8.27 (dd, J_1=8.1 Hz, J_2=2.4 Hz, 1H), 8.12–8.07 (m, 6H), 7.79–7.78 (m, 3H), 7.39 (d, J=8.4 Hz, 1H), 6.55 (s, 1H), 6.41 (s, 1H), 4.31 (s, 3H), 3.99 (s, 3H), 3.96 (s, 3H), 3.89 (s, 3H), 3.87 (s, 3H), 3.39–3.27 (m, 6H), 1.55 (s, 54H), 1.12 (t, J=7.2 Hz, 3H), 1.08 (t, J=7.2 Hz, 3H), −2.70 (s, 1H). ^{13}C NMR (100 MHz, $CDCl_3$): δ 168.0, 164.0, 162.7, 162.2, 157.3, 153.4, 149.0, 148.9, 148.8 (d), 146.2, 146.1, 141.6, 141.5, 139.0, 135.9, 130.2, 130.0, 129.9, 129.8, 125.8, 122.0, 121.6, 121.5, 121.3, 121.1, 121.1, 121.0, 118.7, 115.7, 114.8, 110.1, 95.9, 95.2, 77.5, 56.8, 56.6 (d), 56.2, 43.0, 41.2, 41.0, 35.2, 35.2, 32.0, 14.5, 13.1. MS (MALDI-TOF): m/z 1497 $[M+H]^+$. HRMS (MALDI-FT): Calcd for $C_{94}H_{111}N_8O_9$ $[M+H]^+$: 1495.8452. Found: 1495.8468.

4.13. Compound 29

^{1}H NMR (300 MHz, $CDCl_3$): δ 10.55 (s, 1H), 10.09 (s, 1H), 9.73 (s, 1H), 9.64 (s, 1H), 9.26 (s, 1H), 9.02 (d, J=4.8 Hz, 1H), 8.94–8.92 (m, 6H), 8.80–8.77 (m, 2H), 8.29 (dd, J_1=4.7 Hz, J_2=0.75 Hz, 1H), 8.10–8.08 (m, 6H), 8.01 (s, 1H), 7.80–7.79 (m, 3H), 6.64 (s, 1H), 6.47 (s, 1H), 4.06 (s, 3H), 4.02 (s, 3H), 3.95 (s, 1H), 3.92 (s, 3H), 3.42–3.33 (m, 6H), 1.53 (s, 54H), 1.18–1.09 (m, 6H). ^{13}C NMR (100 MHz, $CDCl_3$): δ 167.9, 163.8, 162.1, 161.7, 154.9, 153.2, 152.5, 149.3, 148.9, 148.7, 146.4, 146.2, 141.3, 141.1, 131.7, 130.0, 129.8, 129.7, 127.8, 125.8, 122.3, 122.0, 121.9, 121.2, 120.5, 115.4, 115.1, 115.0, 95.9, 95.2, 56.6, 56.5, 56.1, 42.8, 41.0, 40.8, 35.1, 31.9, 31.8, 29.7, 14.3, 12.9. MS (MALDI-TOF): m/z 1467.9 $[M+H]^+$. HRMS (MALDI-FT): Calcd for $C_{92}H_{108}N_9O_8$ $[M+H]^+$: 1466.8298. Found: 1466.8315.

4.14. Compound 35

^{1}H NMR (300 MHz, $CDCl_3$): δ 10.55 (s, H), 10.34 (s, 1H), 9.49 (s, 1H), 9.31 (s, 1H), 8.95–8.90 (m, 8H), 8.31 (d, J=8.1 Hz, 1H), 8.22 (s, 1H), 8.15–8.12 (m, 6H), 7.83 (s, 3H), 7.76 (d, J=8.1 Hz, 1H), 7.40 (d, J=8.7 Hz, 1H), 6.92 (d, J=8.7 Hz, 1H), 6.64 (s, 1H), 4.33 (s, 3H), 4.04 (s, 3H), 3.95 (s, 3H), 3.94 (s, 3H), 3.49 (s, 2H), 3.46–3.32 (m, 4H), 1.57 (s, 54H), 1.20 (t, J=6.9 Hz, 3H), 1.14 (t, J=6.9 Hz, 3H), −2.64 (s, 2H). ^{13}C NMR (100 MHz, $CDCl_3$): δ 167.5, 164.6, 164.4, 162.5, 157.1, 151.1, 148.8, 148.6, 148.6, 146.2 (d), 141.5, 141.4, 138.0, 135.7, 130.0, 129.8 (d), 129.6, 127.8, 127.3, 124.7, 121.6, 121.4 (d), 120.9 (d), 118.6, 117.9, 115.6, 110.0, 95.8, 56.7, 56.5, 56.4, 56.1, 42.8, 40.9, 40.9, 35.1 (d), 31.8, 17.6, 14.4, 12.9, 1.0. MS (MALDI-TOF): m/z 1467.2 $[M+H]^+$. MS-HR (MALDI-FT): Calcd for $C_{93}H_{109}N_8O_8$ $[M+H]^+$: 1465.8389. Found: 1465.8363.

4.15. Compound 39

^{1}H NMR (300 MHz, $CDCl_3$): δ 10.60 (s, 1H), 9.53 (s, 1H), 9.30 (d, J=2.4 Hz, 1H), 8.95–8.89 (m, 8H), 8.67 (s, 1H), 8.33 (dd, J_1=8.3 Hz, J_2=2.4 Hz, 1H), 8.29–8.26 (m, 2H), 8.20 (d, J=8.1 Hz, 1H), 8.15–8.11 (m, 6H), 7.83 (s, 3H), 7.59 (t, J=8.1 Hz, 1H), 7.42 (d, J=8.7 Hz, 1H), 6.60 (s, 1H), 4.33 (s, 3H), 4.03 (s, 3H), 3.92 (s, 3H), 1.57 (s, 54H), −2.65 (s, 2H). ^{13}C NMR (100 MHz, $CDCl_3$): δ 160.6, 157.1, 148.9, 148.7, 148.6, 148.2, 146.5, 141.4 (d), 138.6, 138.1, 136.9, 135.9, 133.3, 130.0, 129.8 (d), 129.6, 125.8, 121.9, 121.7, 121.4, 121.0, 120.7, 119.7, 118.4, 115.4, 110.1, 95.4, 77.2, 56.6, 56.5, 56.2, 35.1, 31.8, 31.4, 1.0. MS (MALDI-TOF): m/z 1325.3 $[M+H]^+$. MS-HR (MALDI-TOF-FT): Calcd for $C_{85}H_{94}N_7O_7$ $[M+H]^+$: 1324.7214. Found: 1324.7209.

4.16. Compound 24

To a stirred solution of **23** (0.15 g, 0.10 mmol), C_{60} (72 mg, 0.10 mmol), CBr_4 (33 mg, 0.10 mmol) in toluene (200 mL) was added DBU (33 μL, 37 mg, 0.22 mmol). The solution was stirred for 12 h and then concentrated with a rotavapor. The resulting slurry was subjected to column chromatography (CH_2Cl_2/MeOH, 250:1) to give **24** as a dark brown solid (76 mg, 34%). ^{1}H NMR (300 MHz, $CDCl_3$): δ 10.48 (s, 1H), 9.98 (s, 1H), 9.58 (s, 1H), 9.25 (s, 1H), 8.93–8.87 (m, 8H), 8.60 (s, 1H), 8.27 (d, J=7.8 Hz, 1H), 8.17–8.05 (m, 6H), 7.78 (s, 3H), 7.37 (d, J=8.1 Hz, 1H), 6.46 (s, 1H), 6.20 (s, 1H), 4.29 (s, 3H), 3.97 (s, 3H), 3.84 (s, 6H), 3.61 (s, H), 4.29–3.61 (m, 4H), 1.50 (s, 54H), 1.23 (t, J=6.6 Hz, 3H), 1.14 (t, J=6.6 Hz, 3H), −2.66 (s, 1H). ^{13}C NMR (100 MHz, $CDCl_3$): δ 157.1, 148.8, 148.6, 145.0, 144.1, 144.0, 143.5, 143.2, 143.0, 142.3, 141.9, 141.8, 141.7, 141.5, 141.1, 140.5, 138.4, 130.1, 129.8 (d), 129.6, 121.5, 121.1, 120.9, 110.0, 77.2, 73.6, 56.5, 56.4, 55.9, 42.7, 40.2, 35.1, 31.9, 31.8, 29.7, 13.9, 12.7, 1.0. MS (MALDI-TOF): m/z 2216.8 $[M+H]^+$. HRMS (MALDI-FT): Calcd for $C_{154}H_{109}N_8O_9$ $[M+H]^+$: 2212.8396. Found: 2213.8312.

4.17. Compound 30

^{1}H NMR (300 MHz, $CDCl_3$): δ 10.38 (d, J=2.7 Hz, 1H), 9.97 (s, 1H), 9.55 (s, 1H), 9.09 (s, 1H), 8.94 (d, J=4.8 Hz, 1H), 8.90–8.84 (m, 6H), 8.74–8.73 (m, 2H), 8.29 (d, J=5.7 Hz, 1H), 8.13–8.11 (m, 3H), 8.00–7.96 (m, 4H), 7.75–7.73 (m, 3H), 6.46 (s, 1H), 6.09 (s, 1H), 3.97 (s, 3H), 3.85 (s, 3H), 3.74 (s, 3H), 3.47 (s, 3H), 1.47 (s, 54H), 1.18–1.07 (m, 6H), −2.77 (s, 2H). ^{13}C NMR (100 MHz, $CDCl_3$): δ 162.4, 161.2, 152.4, 148.8, 145.1, 144.2, 144.0, 143.8, 143.3, 143.0, 142.9, 142.3, 142.0, 141.8, 141.7, 141.3, 141.2, 140.3, 138.2, 131.8, 129.8, 129.7, 122.0, 121.8, 121.1, 115.6, 77.3, 56.3, 56.2, 56.0, 55.9, 42.7, 40.3, 35.1, 31.8, 31.8, 31.5, 31.4, 29.7, 29.6, 29.4, 22.7, 14.1, 13.9, 12.8, 1.03. MS (MALDI-TOF): m/z 2186.0 $[M+H]^+$. HRMS (MALDI-FT): Calcd for $C_{152}H_{106}N_9O_8$ $[M+H]^+$: 2184.8163. Found: 2184.8159.

4.18. Compound 36

^{1}H NMR (300 MHz, $CDCl_3$): δ 10.46 (s, 1H), 9.26 (s, 1H), 9.15 (d, J=2.1 Hz, 1H), 9.01 (s, 1H), 8.81–8.73 (m, 9H), 8.15 (dd, J_1=8.3 Hz, J_2=1.8 Hz, 1H), 8.03–8.01 (m, 7H), 7.68–7.65 (m, 4H), 7.28 (d, J=8.7 Hz, 1H), 6.82 (d, J=9.3 Hz, 1H), 6.46 (s, 1H), 4.17 (s, 3H), 3.88 (s, 3H), 3.76 (s, 3H), 3.75 (s, 3H), 4.17–3.75 (m, 2H), 3.44 (s, 2H), 1.42 (s, 54H), 1.15 (t, J=7.5 Hz, 3H), 1.05 (t, J=7.5 Hz, 3H), −2.76 (s, 2H). ^{13}C NMR (100 MHz, $CDCl_3$): δ 164.3, 162.4, 159.8, 157.1, 148.8, 148.6, 143.8, 143.7 (d), 143.6, 143.4, 143.1, 143.0, 142.5, 141.9, 141.7, 141.5, 141.4 (d), 140.7, 140.3, 138.2, 129.9, 129.8, 121.5, 120.9, 118.6, 110.3, 110.1, 95.6, 77.2, 57.9, 56.6, 56.5, 56.3, 56.1, 42.8, 40.4, 35.0, 31.8, 31.6, 29.7, 22.7, 14.1, 13.8, 12.6, 1.0. MS (MALDI-TOF): m/z 2186.2 $[M+H]^+$. HRMS (MALDI-FT): Calcd for $C_{153}H_{107}N_8O_8$ $[M+H]^+$: 2183.8216. Found: 2183.8206.

4.19. Compound 42

^{1}H NMR (300 MHz, $CDCl_3$): δ 10.46 (s, 1H), 10.40 (s, 1H), 9.23 (d, J=1.2 Hz, 1H), 9.05 (s, 1H), 8.92–8.77 (m, 8H), 8.41 (d, J=8.7 Hz, 1H), 8.21–7.79 (m, 13H), 7.51 (d, J=8.1 Hz, 1H), 7.41 (d, J=8.1 Hz, 1H), 6.53 (s, 1H), 4.32 (s, 3H), 4.00 (s, 3H), 3.83 (s, 3H), 3.76–3.31 (m, 4H), 1.04 (t, J=7.2 Hz, 3H), 0.89 (t, J=7.2 Hz, 3H), −2.66 (s, 2H). ^{13}C NMR (100 MHz, $CDCl_3$): δ 148.8, 148.7, 148.6 (d), 144.1, 143.7, 143.5, 143.3, 142.7, 142.6, 141.5 (d), 140.1, 139.9, 137.5, 135.8, 130.0, 129.8, 129.6, 129.5, 121.6, 121.5, 120.9, 56.6, 56.5, 56.2, 33.8, 31.9, 31.8, 30.4, 30.2, 29.7, 29.5, 29.4, 26.7, 22.7, 14.2, 14.1, 13.7, 12.7, 1.0. MS (MALDI-TOF): m/z 2155.4 $[M+H]^+$. HRMS (MALDI-FT): Calcd for $C_{152}H_{105}N_8O_7$ $[M+H]^+$: 2153.8132. Found: 2153.8101.

4.20. Compound 44

^{1}H NMR (300 MHz, $CDCl_3$): δ 10.18 (s, 1H), 10.10 (s, 1H), 9.81 (s, 1H), 9.60 (s, 1H), 8.99 (s, 1H), 8.62 (s, 1H), 8.33 (d, J=7.2 Hz, 1H), 7.89–7.84 (m, 1H), 7.45–7.41 (m, 1H), 6.54 (s, 1H), 6.48 (s 1H), 4.02 (s, 3H), 3.93–3.91 (m, 9H), 3.49–3.37 (m, 6H), 1.25–1.14 (m, 6H). MS (MALDI-TOF): m/z 594.4 $[M+H]^+$. ^{13}C NMR (100 MHz, $CDCl_3$): δ 229.6, 167.9, 163.8, 162.0, 161.4, 154.9, 153.1, 150.8, 147.9, 145.8, 137.4, 130.6, 125.9, 125.6, 122.5, 122.0, 121.2, 120.4, 115.0, 114.6, 95.7, 95.2, 56.6, 56.5, 56.3, 56.1, 42.9, 41.0, 40.9, 29.7, 14.4, 13.0, 1.01.

HRMS (MALDI-FT): Calcd for $C_{30}H_{35}N_5O_8Na$ $[M+Na]^+$: 616.2386. Found: 616.23779.

4.21. Compound 46

^1H NMR (300 MHz, $CDCl_3$): δ 8.80 (s, 1H), 8.05 (s, 1H), 6.50 (s, 1H), 3.92 (s, 6H), 3.84 (s, 3H), 3.49 (s, 4H), 1.53 (s, 2H), 1.26 (s, 2H), 1.18 (s, 6H). MS (EI): m/z 378 $[M]^+$. ^{13}C NMR (100 MHz, $CDCl_3$): δ 168.8, 167.5, 165.5, 157.4, 152.4, 123.3, 120.4, 111.6, 95.7, 56.6, 55.9, 51.7, 31.7, 29.7, 14.4. Anal. Calcd for $C_{19}H_{26}N_2O_8$: C, 60.30; H, 6.93; N, 7.40. Found: C, 60.31; H, 6.94; N, 7.19.

4.22. Compound 9

^1H NMR (300 MHz, $CDCl_3$): δ 9.03 (s, 1H), 8.92 (s, 1H), 6.58 (s, 1H), 4.03 (s, 3H), 3.96 (s, 3H), 3.89 (s, 3H), 4.03–3.89 (m, 4H), 1.40 (t, J=7.2 Hz, 3H), 1.30 (t, J=7.2 Hz, 3H). ^{13}C NMR (100 MHz, $CDCl_3$): δ 165.6, 162.7, 159.6, 158.2, 153.3, 145.2 (d), 144.9, 144.7, 144.6, 143.9, 143.1, 143.0 (d), 142.9, 142.3, 142.2 (d), 141.1, 141.0, 139.0, 124.0, 119.9, 111.9, 95.9, 77.2, 58.3, 56.7, 56.2, 51.9, 43.0, 40.5, 13.9, 12.8, 1.0. MS (MALDI-TOF): m/z 1093.3 $[M+Na]^+$. HRMS (MALDI-FT): Calcd for $C_{77}H_{22}N_2O_6Na$ $[M+Na]^+$. 1093.1330. Found: 1093.1370.

4.23. Compound 1

To a stirred solution of **24** (10.0 mg, 0.0045 mmol) in CH_2Cl_2 (50 mL) was added a solution of zinc acetate (8.0 mg, 0.045 mmol) in MeOH (3 mL). The solution was stirred for 12 h and then concentrated with a rotavapor. The resulting slurry was triturated with CH_2Cl_2 (50 mL) and the organic phase washed with saturated aqueous $NaHCO_3$ (25 mL), water (25 mL) and brine (25 mL), and dried over sodium sulfate. The solvent was then removed under reduced pressure to afford **1** as a purple solid (8.5 mg, 82%). ^1H NMR (300 MHz, $CDCl_3$): δ 10.41 (s, 1H), 9.89 (s, 1H), 9.49 (s, 1H), 9.14 (s, 1H), 8.96–8.88 (m, 8H), 8.48 (s, 1H), 8.21 (d, J=8.4 Hz, 1H), 8.11–7.97 (m, 7H), 7.72–7.72 (m, 3H), 7.26 (d, J=8.4 Hz, 1H), 6.34 (s, 1H), 6.07 (s, 1H), 4.21 (s, 3H), 3.87 (s, 3H), 3.74 (s, 3H), 3.72 (s, 3H), 3.499 (s, 3H), 4.21–3.49 (m, 4H), 1.47 (s, 54H), 1.11 (t, J=7.2 Hz, 3H), 1.04 (t, J=7.2 Hz, 3H). ^{13}C NMR (100 MHz, $CDCl_3$): δ 162.3, 161.3, 156.9, 150.6, 150.5 (d), 150.3, 148.6, 148.5, 148.4, 145.0, 144.0, 143.9 (d), 142.9, 142.8, 142.3, 142.2, 142.1, 141.7 (d), 141.0, 140.4, 140.3, 136.4, 135.8, 132.3 (d), 132.2, 131.8 (d), 129.9, 129.8, 129.6, 128.3, 125.5, 122.6, 122.5, 121.8, 120.7, 119.7, 56.5, 56.3, 35.1, 34.2, 32.8, 31.9 (t), 31.8, 30.2, 29.7 (d), 29.5, 27.1, 23.2, 22.7, 14.2, 14.1, 13.9, 12.7. MS (MALDI-TOF): m/z 2279.0 $[M+H]^+$. HRMS (MALDI-FT): Calcd for $C_{154}H_{106}N_8O_9Zn$ $[M+H]^+$: 2274.7448. Found: 2274.7369.

4.24. Compound 2

^1H NMR (300 MHz, $CDCl_3$): δ 10.41 (s, 1H), 9.95 (s, 1H), 9.56 (s, 1H), 9.08 (s, 1H), 8.97–8.94 (m, 7H), 8.83–8.82 (m, 2H), 8.45 (s, 1H), 8.28 (d, J=4.8 Hz, 1H), 8.12–8.10 (m, 3H), 8.00–7.96 (m, 4H), 7.73 (s, 3H), 6.50 (s, 1H), 6.17 (s, 1H), 3.98 (s, 3H), 3.86 (s, 3H), 3.79 (s, 3H), 3.55 (s, 3H), 1.47 (s, 54H), 0.87–0.75 (m, 6H). ^{13}C NMR (100 MHz, $CDCl_3$): δ 150.9, 150.7, 150.5, 148.9, 148.7, 148.5, 145.1, 143.8, 142.9, 142.3, 142.0, 141.9, 141.7, 140.3, 138.3, 132.6, 132.4, 129.8, 129.7, 129.6, 122.9, 120.9, 77.3, 71.5, 71.0, 61.8, 56.1, 35.1, 31.9, 31.8, 31.7, 29.7, 19.3, 14.1, 14.0, 13.9, 12.8. MS (MALDI-TOF): m/z 2250.5 $[M+H]^+$. MS-HR (MALDI-FT) Calcd for $C_{152}H_{103}N_9O_8Zn$ $[M+H]^+$: 2245.7171. Found: 2245.7216.

4.25. Compound 3

^1H NMR (300 MHz, $CDCl_3$): δ 10.59 (s, 1H), 9.30 (s, 1H), 9.19 (d, J=2.1 Hz, 1H), 9.14 (s, 1H), 9.01–8.92 (m, 8H), 8.82 (s, 1H), 8.31 (dd, J_1=8.3 Hz, J_2=1.8 Hz, 1H), 8.14–8.09 (m, 7H), 8.14–8.09 (m, 4H), 7.42 (d, J=8.4 Hz, 1H), 7.07 (s, 1H), 6.59 (s, 1H), 4.33 (s, 3H), 4.03 (s, 3H), 3.92 (s, 3H), 3.89 (s, 3H), 3.57 (s, 4H), 1.53 (s, 54H), 1.11 (t, J=7.2 Hz, 3H), 1.04 (t, J=7.2 Hz, 3H). ^{13}C NMR (100 MHz, $CDCl_3$): δ 162.5, 162.4, 156.9, 150.4 (d), 150.2, 148.5, 148.3, 143.8, 143.7, 143.2, 143.1, 143.0, 142.1, 141.9, 141.5, 140.3, 138.3, 132.3, 132.1 (d), 131.6, 129.8, 129.6, 125.5, 122.4, 120.6, 110.3, 57.9, 56.6, 56.5, 56.3, 56.1, 42.8, 40.4, 35.0, 31.9, 31.8, 30.3, 30.2, 29.7, 29.5, 29.4, 29.3, 29.0, 26.7, 23.2, 22.7, 14.2, 14.1, 13.8, 12.6, 1.0. MS (MALDI-TOF): m/z 2246.7 $[M]^+$. HRMS (MALDI-FT): Calcd for $C_{153}H_{104}N_8O_8Zn$ $[M+H]^+$: 2244.7228. Found: 2244.7263.

4.26. Compound 4

^1H NMR (300 MHz, $CDCl_3$): δ 10.42 (s, 1H), 10.23 (s, 1H), 9.15 (s, 1H), 8.99–8.85 (m, 9H), 8.46 (d, J=7.2 Hz, 1H), 8.22–8.10 (m, 4H), 7.98 (s, 3H), 7.82–7.76 (m, 6H), 7.47–7.41 (m, 2H), 6.54 (s, 1H), 4.34 (s, 3H), 4.02 (s, 3H), 3.83 (s, 3H), 3.29 (s, 4H), 1.15 (t, J=7.5 Hz, 3H), 1.00 (t, J=7.5 Hz, 3H). ^{13}C NMR (100 MHz, $CDCl_3$): δ 161.7, 160.2, 156.7, 150.4 (d), 150.2, 148.4, 148.3 (d), 142.5, 142.1, 142.0, 141.4, 140.0, 139.8, 137.4, 132.3, 132.2 (d), 131.6, 129.9, 129.7, 129.4, 129.1, 125.3, 122.4, 120.6, 109.6, 95.2, 58.0, 56.5, 56.4, 56.0, 42.2, 39.8, 35.5, 35.0, 31.8, 29.7, 29.6, 29.5, 29.3 (d), 29.2, 29.1, 29.0, 25.2, 23.2, 22.7, 14.2, 13.7, 12.7, 1.0. MS (MALDI-TOF): m/z 2155 $[M+K]^+$. HRMS (MALDI-FT): Calcd for $C_{152}H_{102}N_8O_7Zn$ $[M]^+$: 2214.7178. Found: 2214.7158.

4.27. Compound 5

^1H NMR (300 MHz, $CDCl_3$): δ 10.43 (s, 1H), 10.00 (s, 1H), 9.62 (s, 1H), 9.45 (s, 1H), 9.25 (d, J=2.7 Hz, 1H), 9.03–8.96 (m, 8H), 8.84 (s, 1H), 8.30 (dd, J_1=8.3 Hz, J_2=2.4 Hz, 1H), 8.12–8.07 (m, 6H), 7.79–7.78 (m, 3H), 7.40 (d, J=8.4 Hz, 1H), 6.58 (s, 1H), 6.43 (s, 1H), 4.33 (s, 3H), 4.00 (s, 3H), 3.98 (s, 3H), 3.90 (s, 3H), 3.88 (s, 3H), 3.34 (s, 2H), 3.31–3.26 (m, 4H), 1.53 (s, 54H), 1.108 (t, J=7.2 Hz, 3H), 1.039 (t, J=7.2 Hz, 3H). ^{13}C NMR (100 MHz, $CDCl_3$): δ 167.7, 163.8, 162.6, 157.0, 155.0, 150.5, 150.4 (d), 150.3, 148.6, 148.5 (d), 148.4, 145.9, 142.1, 142.0, 137.9, 136.3, 132.4, 132.1, 132.0, 131.8, 130.0, 129.7, 129.6, 122.4, 121.2, 120.8, 120.7, 115.5, 114.6, 109.8, 95.8, 95.1, 78.1, 78.0 (d), 77.9, 77.8, 56.6, 56.5, 56.4, 56.0, 42.8, 40.9, 40.7, 35.1, 35.0, 31.8 (d), 31.5 (d), 29.7, 14.3, 12.8. MS (MALDI-TOF): m/z 1560.1 $[M+H]^+$. HRMS (MALDI-FT): Calcd for $C_{94}H_{108}N_8O_9ZnNa$ $[M+Na]^+$: 1579.7472. Found: 1579.7423.

4.28. Compound 6

^1H NMR (300 MHz, $CDCl_3$): δ 10.60 (s, 1H), 10.15 (s, 1H), 9.74 (s, 1H), 9.65 (s, 1H), 9.18 (s, 1H), 9.01–8.97 (m, 6H), 8.88 (s, 1H), 8.83–8.82 (m, 2H), 8.32 (d, J=4.8 Hz, 1H), 8.08 (s, 7H), 7.78 (s, 3H), 7.63 (s, 1H), 6.60 (s, 1H), 6.44 (s, 1H), 4.05 (s, 3H), 4.00 (s, 3H), 3.93 (s, 3H), 3.89 (s, 3H), 3.39–3.27 (m, 6H), 1.15–1.06 (m, 6H). ^{13}C NMR (100 MHz, $CDCl_3$): δ 167.8, 163.8, 162.0, 161.9, 154.9, 150.6, 150.4, 150.3, 148.9, 148.8, 148.5, 148.4, 146.2, 146.0, 143.6, 142.2, 142.1, 132.9, 132.2, 132.0, 130.7, 129.9, 129.8, 129.7, 128.0, 122.5, 122.4, 120.7, 116.0, 114.8, 95.8, 95.2, 71.5, 56.5, 56.1, 49.3, 42.8, 40.9, 40.8, 36.4, 35.0, 31.8, 31.5, 31.3, 30.2, 29.7, 19.3, 17.5, 14.3, 13.9, 12.9. MS (MALDI-TOF): m/z 1530.0 $[M+H]^+$. HRMS (MALDI-FT): Calcd for $C_{92}H_{105}N_9O_8ZnNa$ $[M+Na]^+$: 1550.7163. Found: 1550.72698.

4.29. Compound 7

^1H NMR (300 MHz, $CDCl_3$): δ 10.55 (s, 1H), 10.12 (s, 1H), 9.45 (s, 1H), 9.26 (d, J=1.8 Hz, 1H), 9.02–8.96 (m, 8H), 8.83 (s, 1H), 8.30 (dd, J_1=8.1 Hz, J_2=1.8 Hz, 1H), 8.18 (s, 1H), 8.13–8.11 (m, 6H), 7.81 (s, 3H), 7.73 (dd, J_1=8.1 Hz, J_2=1.5 Hz, 1H), 7.39 (d, J=8.7 Hz, 1H), 6.90 (d, J=9H, 1H), 6.61 (s, 1H), 4.33 (s, 3H), 4.03 (s, 3H), 3.93 (s, 3H), 3.89 (s, 3H), 3.34–3.17 (m, 6H), 1.56 (s, 54H), 1.15 (t, J=7.2 Hz, 3H), 1.06 (t, J=7.2 Hz, 3H). MS (MALDI-TOF): m/z 1529 $[M]^+$. ^{13}C NMR (100 MHz, $CDCl_3$): δ 167.4, 164.4 (d), 162.6, 156.9, 150.5, 150.4, 150.3, 148.6,

148.5, 148.4 (d), 146.1, 142.1, 142.0, 136.4, 132.4, 132.1, 132.0, 131.7, 129.9, 129.7, 129.6, 127.8, 127.2, 124.7, 122.3, 120.9, 120.7, 117.9, 110.0, 109.9, 95.8, 56.7, 56.5, 56.4, 56.1, 53.4, 49.2, 42.7, 40.8, 35.1, 35.0, 31.8, 31.6, 31.5, 29.8, 29.7, 28.9, 17.4, 14.3, 12.8, 1.0. HRMS (MALDI-FT): Calcd for $C_{93}H_{106}N_8O_8Zn$ $[M]^+$: 1526.7457. Found: 1526.7420.

4.30. Compound 8

^{1}H NMR (300 MHz, $CDCl_3$): δ 10.50 (s, 1H), 9.24 (s, 1H), 9.09 (s, 1H), 9.01–8.90 (m, 8H), 8.77 (s, 1H), 8.32 (s, 1H), 8.29 (s, 1H), 8.12–8.10 (m, 6H), 7.79 (s, 3H), 7.62 (s, 1H), 7.58 (d, J=7.2 Hz, 1H), 7.36 (d, J=8.4 Hz, 1H), 7.22 (d, J=8.4 Hz, 1H), 6.49 (s, 1H), 4.29 (s, 3H), 3.98 (s, 3H), 3.81 (s, 3H), 2.71 (d, J=6.6 Hz, 2H), 2.47 (d, J=6.6 Hz, 2H), 0.72 (t, J=6.9 Hz, 3H), 0.61 (t, J=6.9 Hz, 3H). ^{13}C NMR (100 MHz, $CDCl_3$): δ 166.6, 164.9, 163.4, 162.6, 156.9, 150.4, 150.3, 150.2 (d), 148.5, 148.4 (d), 142.3, 142.2, 138.0, 135.8, 132.3, 132.0 (d), 131.6, 129.9, 129.8, 129.7, 129.1, 123.3, 122.2, 121.3, 120.6, 120.4, 117.9, 109.8, 95.6, 56.6, 56.4, 56.1, 42.2, 40.2, 38.0, 35.0, 31.8, 31.5, 29.7, 14.0, 12.4. MS (MALDI-TOF): m/z 1500.2 $[M+H]^+$. HRMS (MALDI-FT): Calcd for $C_{92}H_{105}N_8O_7Zn$ $[M+H]^+$: 1497.7436. Found: 1497.7392.

4.31. Compound 32

A solution of **18** (1.19 g, 12.0 mmol), **31** (2.17 g, 12.0 mmol) and DCC (2.97 g, 14.4 mmol) in CH_2Cl_2 (50 mL) was stirred for 12 h and then washed with diluted aqueous HCl (0.1 N, 25 mL), water (25 mL) and brine (25 mL), and dried over sodium sulfate. The solvent was removed and the resulting slurry subjected to flash chromatography (CH_2Cl_2/MeOH 100:1) to give **32** as a pale grey solid (2.49 g, 63%). ^{1}H NMR (300 MHz, $CDCl_3$): δ 10.35 (s, 1H), 8.99 (s, 1H), 7.82 (d, J=9.9 Hz, 1H), 6.92 (d, J=8.4 Hz, 1H), 3.98 (s, 3H), 3.88 (s, 3H), 3.49 (s, 2H), 3.47–3.37 (m, 4H), 1.24 (t, J=7.5 Hz, 3H), 1.170 (t, J=7.5 Hz, 3H). ^{13}C NMR (100 MHz, $CDCl_3$): δ 167.5, 166.9, 164.4, 152.3, 127.3, 126.4, 122.8, 121.4, 109.5, 56.1, 51.9, 42.8, 40.9 (d), 14.4, 12.9. MS (EI): m/z 322 $[M]^+$. Anal. Calcd for $C_{16}H_{22}N_2O_5$: C, 59.61; H, 6.88; N, 8.69. Found: C, 59.38; H, 7.05; N, 8.33.

4.32. Compound 33

A solution of **32** (0.26 g, 0.82 mmol) and lithium hydroxide monohydrate (0.34 g, 8.19 mmol) in THF (5 mL) and MeOH (5 mL) was stirred for 2 h and then concentrated. The resulting slurry was triturated with $CHCl_3$ (20 mL). After workup, the crude product was recrystallized from MeOH to give **33** as a white solid (0.19 g, 76%). ^{1}H NMR (300 MHz, CD_3OD): δ 8.81 (d, J=1.8 Hz, 1H), 7.81 (dd, J_1=1.8 Hz, J_2=8.7 Hz, 1H), 7.08 (d, J=8.7 Hz, 1H), 3.96 (s, 3H), 3.62 (s, 2H), 3.49–3.39 (m, 4H), 1.23 (t, J=7.2 Hz, 3H), 1.15 (t, J=7.2 Hz, 3H). ^{13}C NMR (100 MHz, $CDCl_3$): δ 169.9, 169.4, 167.9, 154.9, 128.6, 128.5, 124.4, 124.1, 83.2, 57.0, 14.7, 13.4. MS (ESI): m/z 309.1 $[M+H]^+$. Anal. Calcd for $C_{15}H_{20}N_2O_5$: C, 58.43; H, 6.54; N, 9.09. Found: C, 57.93; H, 6.33; N, 8.87.

4.33. Compound 34

A solution of **21** (0.19 g, 1.10 mmol), **33** (0.31 g, 1.00 mmol), EDCI (0.21 g, 1.10 mmol) and DMAP (2 mg) in $CHCl_3$ (5 mL) was stirred for 12 h and then washed with water (5 mM×2) and brine (5 mL), and dried over sodium sulfate. Upon removal of the solvent with a rotavapor, the resulting residue was subjected to flash chromatography (CH_2Cl_2/MeOH 50:1) to give **34** as a pale yellow solid (0.29 g, 64%). ^{1}H NMR (300 MHz, $CDCl_3$): δ 10.49 (s, 1H), 8.91 (d, J=2.4 Hz, 1H), 8.36 (s, 1H), 7.99 (s, 1H), 7.73 (dd, J_1=8.6 Hz, J_2=2.1 Hz, 1H), 6.98 (d, J=8.4 Hz, 1H), 6.51 (s, 1H), 3.99 (s, 3H), 3.89 (s, 3H), 3.86 (s, 3H), 3.62 (s, 2H), 3.51 (s, 2H), 3.48–3.37 (m, 4H), 1.25 (t, J=7.2 Hz, 3H), 1.19 (t, J=7.2 Hz, 3H). ^{13}C NMR (100 MHz, $CDCl_3$): δ 167.6, 164.4, 164.5, 151.2, 143.3, 141.6, 129.7, 127.9, 127.6, 124.2, 121.8, 118.1, 110.0, 108.3, 97.3, 57.1, 56.2, 56.1, 42.8, 41.0, 40.9, 14.4, 13.0. MS (MALDI-TOF): m/z 459 $[M+H]^+$. HRMS (MALDI-FT): Calcd for $C_{23}H_{30}N_4O_6Na$ $[M+Na]^+$: 481.2074. Found: 481.2058.

4.34. Compound 38

^{1}H NMR (300 MHz, $CDCl_3$): δ 8.70 (s, 1H), 8.41 (s, 1H), 8.38 (s, 1H), 8.23 (d, J=7.5 Hz, 1H), 7.97 (s, 1H), 7.70 (t, J=8.4 Hz, 1H), 6.53 (s, 1H), 3.90 (s, 3H), 3.88 (s, 3H), 3.65 (s, 2H). ^{13}C NMR (100 MHz, $CDCl_3$): δ 141.6, 137.2, 133.0, 130.0, 126.0, 121.9, 120.6, 108.2, 96.7, 56.8, 56.1. MS (ESI): m/z 318 $[M+H]^+$. HRMS (MALDI-FT): Calcd for $C_{15}H_{16}N_3O_5$ $[M+H]^+$: 318.1083. Found: 318.1085.

4.35. Compound 40

A suspension of **39** (0.82 g, 0.62 mol) and Raney Ni (0.10 g) in THF was stirred under the bubble of hydrogen gas for 4 h and then filtrated. The filtrate was concentrated to give **40** as a purple solid (0.80 g, 100%). ^{1}H NMR (300 MHz, $CDCl_3$): δ 10.54 (s, 1H), 9.48 (s, 1H), 9.27 (d, J=2.7 Hz, 1H), 8.92–8.87 (m, 7H), 8.30 (dd, J_1=8.7 Hz, J_2=1.8 Hz, 1H), 8.12–8.08 (m, 6H), 7.80 (s, 3H), 7.49 (d, J=8.4 Hz, 1H), 7.20–7.15 (m, 3H), 6.99 (s, 1H), 6.74 (t, J=2.4 Hz, 1H), 6.62 (s, 1H), 4.34 (s, 3H), 4.04 (s, 3H), 3.92 (s, 3H), 3.78 (s, 2H), 1.54 (s, 54H), −2.68 (s, 2H). ^{13}C NMR (100 MHz, $CDCl_3$): δ 62.6, 157.1, 148.8, 148.7, 148.6 (d), 146.8, 141.4 (d), 140.0, 138.0, 135.8, 130.0, 129.8 (d), 129.6, 129.3, 125.5, 121.7, 121.4, 120.9, 120.8, 120.7, 117.8, 116.5, 115.6, 114.1, 110.0, 95.7, 78.8, 56.7, 56.5, 56.3, 35.1, 34.9, 31.8, 30.4, 29.7, 29.5, 23.9, 1.0. MS (MALDI-TOF): m/z 1295.8 $[M+H]^+$. HRMS (MALDI-FT): Calcd for $C_{85}H_{96}N_7O_5$ $[M+H]^+$: 1294.7486. Found: 1294.7467.

Acknowledgements

We thank the National Natural Science Foundation of China (Nos. 20621062, 20672137, 20732007, and 20872167), the National Basic Research Program (2007CB808001) and the Science and Technology Commission of Shanghai Municipality (09XD1405300) for financial support.

References and notes

1. (a) Gust, D.; Moore, T. A.; Moore, A. L. *Acc. Chem. Res* **2001**, *34*, 40–48; (b) Schuster, D. I. *Carbon* **2000**, *38*, 1607–1614; (c) Santos, J.; Illescas, B. M.; Wielopolski, M.; Silva, A. M. G.; Tome, A. C.; Guldi, D. M.; Martin, N. *Tetrahedron* **2008**, *64*, 11404–11408; (d) Li, Y.; Gan, Z.; Wang, N.; He, X.; Li, Y.; Wang, S.; Liu, H.; Araki, Y.; Ito, O.; Zhu, D. *Tetrahedron* **2006**, *62*, 4285–4293.
2. (a) Guldi, D. M. *Pure Appl. Chem* **2003**, *75*, 1069–1075; (b) Imahori, H. *Org. Biomol. Chem* **2004**, *2*, 1425–1433.
3. Boyd, P. D. W.; Hodgson, M. C.; Rickard, C. E. F.; Oliver, A. G.; Chaker, L.; Brothers, P. J.; Bolskar, R. D.; Tham, F. S.; Reed, C. A. *J. Am. Chem. Soc* **1999**, *121*, 10487–10495.
4. Olmstead, M. M.; Costa, D. A.; Maitra, K.; Noll, B. C.; Phillips, S. L.; Van Calcar, P. M.; Balch, A. L. *J. Am. Chem. Soc* **1999**, *121*, 7090–7097.
5. Schuster, D. I.; Jarowski, P. D.; Kirschner, A. N.; Wilson, S. R. *J. Mater. Chem* **2002**, *12*, 2041–2047.
6. Imahori, H.; Hagiwara, K.; Aoki, M.; Akiyama, T.; Taniguchi, S.; Okada, T.; Shirakawa, M.; Sakata, Y. *J. Am. Chem. Soc* **1996**, *118*, 11771–11782.
7. Bourgeois, J.-P.; Diederich, F.; Echegoyen, L.; Nierengarten, J.-F. *Helv. Chim. Acta* **1998**, *81*, 1835–1844.
8. Dietel, E.; Hirsch, A.; Eichhorn, E.; Rieker, A.; Hackbarth, S.; Roder, B. *Chem. Commun* **1998**, 1981–1982.
9. Schuster, D. I.; Cheng, P.; Jarowski, P. D.; Guldi, D. M.; Luo, C.; Echegoyen, L.; Pyo, S.; Holzwarth, A. R.; Braslavsky, S. E.; Williams, R. M.; Klihm, G. *J. Am. Chem. Soc* **2004**, *126*, 7257–7270.
10. Gadde, S.; Islam, D. M. S.; Wijesinghe, C. A.; Subbaiyan, N. K.; Zandler, M. E.; Araki, Y.; Ito, O.; D'Souza, F. *J. Phys. Chem. C* **2007**, *111*, 12400–12503.
11. Watanabe, N.; Kihara, N.; Forusho, Y.; Takata, T.; Araki, Y.; Ito, O. *Angew. Chem., Int. Ed.* **2003**, *42*, 681–683.
12. Solladie, N.; Walther, M. E.; Gross, M.; Figueira, D.; Teresa, M.; Bourgogne, C.; Nierengarten, J.-F. *Chem. Commun.* **2003**, 2412–2413.
13. Sasabe, H.; Kihara, N.; Forusho, Y.; Mizuno, K.; Ogawa, A.; Takata, T. *Org. Lett.* **2004**, *6*, 3957–3960.
14. Li, K.; Schuster, D. I.; Guldi, D. M.; Herranz, M. A.; Echegoyen, L. *J. Am. Chem. Soc.* **2004**, *126*, 3388–3389.
15. *Foldamers: Structure, Properties and Applications*; Hecht, S., Huc, I., Eds.; Wiley-VCH: Weinheim, Germany, 2007.

16. (a) Gellman, S. H. *Acc. Chem. Res* **1998**, *31*, 173–180; (b) Hill, D. J.; Mio, M. J.; Prince, R. B.; Hughes, T. S.; Moore, J. S. *Chem. Rev* **2001**, *101*, 3893–4011; (c) Gong, B. *Chem.—Eur. J* **2001**, *7*, 4336–4342; (d) Huc, I. *Eur. J. Org. Chem* **2004**, 17–29; (e) Goodman, C. M.; Choi, S.; Shandler, S.; DeGrado, W. F. *Nat. Chem. Biol* **2007**, *3*, 252–262.
17. (a) Li, Z.-T.; Hou, J.-L.; Li, C.; Yi, H.-P. *Chem. Asian J.* **2006**, *1*, 766–778; (b) Li, Z.-T.; Hou, J.-L.; Li, C. *Acc. Chem. Res.* **2008**, *41*, 1343–1353.
18. Ramos, A. M.; Meskers, S. C. J.; Beckers, E. H. A.; Prince, R. B.; Brunsveld, L.; Janssen, R. A. J. *J. Am. Chem. Soc.* **2004**, *126*, 9630–9644.
19. Davis, J. M.; Tsoub, L. K.; Hamilton, A. D. *Chem. Soc. Rev.* **2007**, *36*, 326–334.
20. (a) Hou, J.-L.; Shao, X.-B.; Chen, G.-J.; Zhou, Y.-X.; Jiang, X.-K.; Li, Z.-T. *J. Am. Chem. Soc.* **2004**, *126*, 12386–12394; (b) Wu, Z.-Q.; Shao, X.-B.; Li, C.; Hou, J.-L.; Wang, K.; Jiang, X.-K.; Li, Z.-T. *J. Am. Chem. Soc.* **2005**, *127*, 17460–17468; (c) Li, C.; Ren, S.-F.; Hou, J.-L.; Yi, H.-P.; Zhu, S.-Z.; Jiang, X.-K.; Li, Z.-T. *Angew. Chem., Int. Ed.* **2005**, *44*, 5725–5729; (d) Yi, H.-P.; Li, C.; Hou, J.-L.; Jiang, X.-K.; Li, Z.-T. *Tetrahedron* **2005**, *61*, 7974–7980; (e) Wu, Z.-Q.; Li, C.-Z.; Feng, D.-J.; Jiang, X.-K.; Li, Z.-T. *Tetrahedron* **2006**, *62*, 11054–11062; (f) Du, P.; Xu, Y.-X.; Jiang, X.-K.; Li, Z.-T. *Sci. China, Ser. B Chem.* **2009**, *52*, 489–496.
21. Garric, J.; Léger, J.-M.; Huc, I. *Angew. Chem., Int. Ed.* **2005**, *44*, 1954–1958.
22. Yin, H.; Hamilton, A. D. *Angew. Chem., Int. Ed.* **2005**, *44*, 4130–4163.
23. Wolffs, M.; Delsuc, N.; Veldman, D.; Anh, N. V.; Williams, R. M.; Meskers, S. C. J.; Janssen, R. A. J.; Huc, I.; Schenning, A. P. H. J. *J. Am. Chem. Soc.* **2009**, *131*, 4819–4829.
24. Filler, R.; Lin, S.; Zhang, Z. *J. Fluorine Chem.* **1995**, *74*, 69–76.
25. Plater, M. J.; Aiken, S.; Bourhill, G. *Tetrahedron* **2002**, *58*, 2405–2413.
26. Salom-Roig, X. J.; Chambron, J.-C.; Goze, C.; Heitz, V.; Sauvage, J.-P. *Eur. J. Org. Chem.* **2002**, 3276–3280.
27. Zhu, J.; Parra, R. D.; Zeng, H.; Skrzypczak-Jankun, E.; Zeng, X. C.; Gong, B. *J. Am. Chem. Soc.* **2000**, *122*, 4219–4220.
28. Fernandez, M. V.; Durante-Lanes, P.; Lopez-Herrera, F. J. *Tetrahedron* **1990**, *46*, 7911–7922.
29. Hamuro, Y.; Geib, S. J.; Hamilton, A. D. *J. Am. Chem. Soc.* **1997**, *119*, 10587–10593.
30. Camps, X.; Hirsch, A. *J. Chem. Soc., Perkin Trans. 1* **1997**, 1595–1596.
31. Anderson, J. L.; An, Y.-Z.; Rubin, Y.; Foote, C. S. *J. Am. Chem. Soc.* **1994**, *116*, 9763–9764.
32. Vail, S. A.; Schuster, D. I.; Guldi, D. M.; Isosomppi, M.; Tkachenko, N.; Lemmetyinen, H.; Palkar, A.; Echegoyen, L.; Chen, X.; Zhang, J. Z. H. *J. Phys. Chem. B* **2006**, *110*, 14155–14166.
33. Marcus, R. A. *Angew. Chem., Int. Ed. Engl.* **1993**, *32*, 1111–1121.